Chapter 3: Studies of Partial Agonist Interactions in the Binding Site of Glutamate Receptors using Unnatural Amino Acid Mutagenesis

3.1 Introduction

Ionotropic glutamate receptors are multi-subunit, allosteric, ligand-gated ion channels (LGICs) that undergo agonist-induced conformational changes between an open and closed state. Early studies of many LGICs have demonstrated a step-wise mechanism that controls this conformational change. One intriguing feature of many LGICs is that the relatively small neurotransmitter generally binds in an extracellular domain, often 50Å away from the channel pore. The ensuing conformational changes required to transmit the signal of agonist binding to ion channel gating span a large distance and alter the conformation of a large, multi-subunit protein complex. Exploration of how the binding of a small molecule triggers these structural changes remains a topic of great interest. Structural studies such as x-ray crystallography and NMR spectroscopy are commonly employed to gather molecular level details of these interactions. However, information is sparse due to the difficulty of using these methods on full-length transmembrane receptors. Another approach utilizes chemistry-based methods to obtain information about receptor structure, often by varying the structure of the ligand and/or varying the structure of the receptor by mutagenesis. This method is useful in that full-length receptors are studied and generate results using many structure-function assays. We will employ the second method, utilizing functional, full-length glutamate receptors in concert with several agonists and partial agonists to create a novel functional assay of ligand binding in ionotropic glutamate receptors.

α-amino-3-hydroxy-5-methyl-4-isoxazolepropionic acid **(**AMPA) and N-methyl-D–aspartate (NMDA) receptors are the two main types of glutamate-gated ion channels that couple the energy of glutamate binding to the ligand-binding domain with the opening of the transmembrane ion channel domain (*1*). AMPA receptors mediate most of the fast excitatory neurotransmission in the mammalian brain upon glutamate activation. NMDA receptors play a unique role as ligand-gated ion channels as they require the

binding of both glutamate and glycine to couple to ion channel function and membrane depolarization for release of the magnesium block (*2*). The prerequisite for both chemical and electrical stimuli, coupled with the calcium permeability of NMDA receptors, establishes the key differences between them and the other ionotropic glutamate receptor (iGluR) subtypes (Figure 3.1). Although members of the the iGluR family have unique biological roles, they are all implicated in learning and memory under normal conditions and several disease states (including stroke, schizophrenia, and neurodegenerative diseases), and identifying agonists that modulate their function could be a useful treatment strategy (*3-5*).

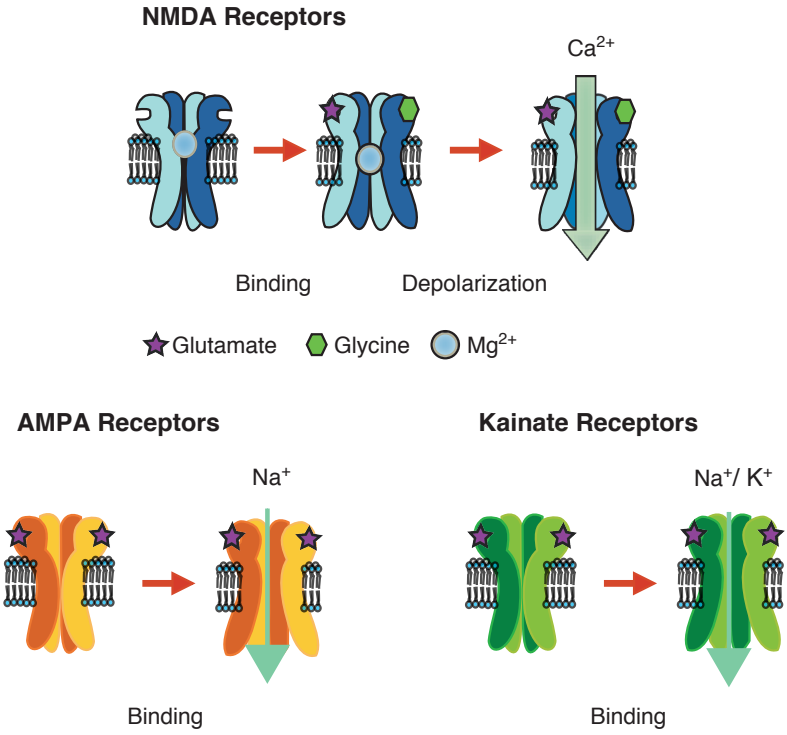

Figure 3.1 iGluR Familes, NMDARs, AMPARs, and KA Receptors.

The goal is to determine the interactions that guide the binding of glutamate to these different receptors and map the interactions that remain conserved across the family and the interactions that are different between NMDA and AMPA receptors. In particular, we want to identify the chemical-scale interactions that influence the NMDA NR1 subunit preference for glycine and the NR2 subunit preference for glutamate. Our

studies will begin by focusing on the NR2 ligand-binding domain and its interactions with several agonists.

3.1.1 The Mechanism of Partial Agonist Action on Glutamate Receptors

Direct structural studies of full-length ion channels remain elusive, yet recent studies have developed "tricks" to gain insight into these complicated transmembrane proteins. Since 1998, a plethora of structural evidence for ligand interaction with the ligand-binding domain of iGluRs has erupted. A methodology developed by Gouaux and co-workers enabled the generation of high-resolution crystal structures of the ligand-binding domain (LBD) of all types (AMPA, NMDA, and Kainate) of iGluRs in complex with agonists, partial agonists, and antagonists (*6*). These structural studies have provided many insights into the mechanism of agonist interactions with the different iGluR subtypes. Additionally, crystal structures of many iGluR LBDs in complex with partial agonists have provided insight into the mechanism of partial agonism of iGluRs. Another important result of many of these studies is that although the iGluRs have structural similarities in overall topology and specifically in their LBDs, there are many subtle underlying differences between the subtypes within a family (e.g., GluR2 vs. GluR4) and between families (e.g., AMPAR vs. NMDAR).

These structural studies are incredibly useful because they provide direct images of the LBD from mammalian iGluRs, however they are not the full-length receptors and do not directly correlate to functional representations of iGluR LBDs. These caveats are important to remember when constructing hypotheses and conclusions about the function of iGluRs that are solely based on these structural images. Additionally, it is important to remember that differences exist between iGluR subtypes, and the conclusions made regarding one type of receptor will not always translate to another subtype. Nevertheless, these crystal structures form a basis for our investigations into the mechanism of agonist action with full-length iGluRs.

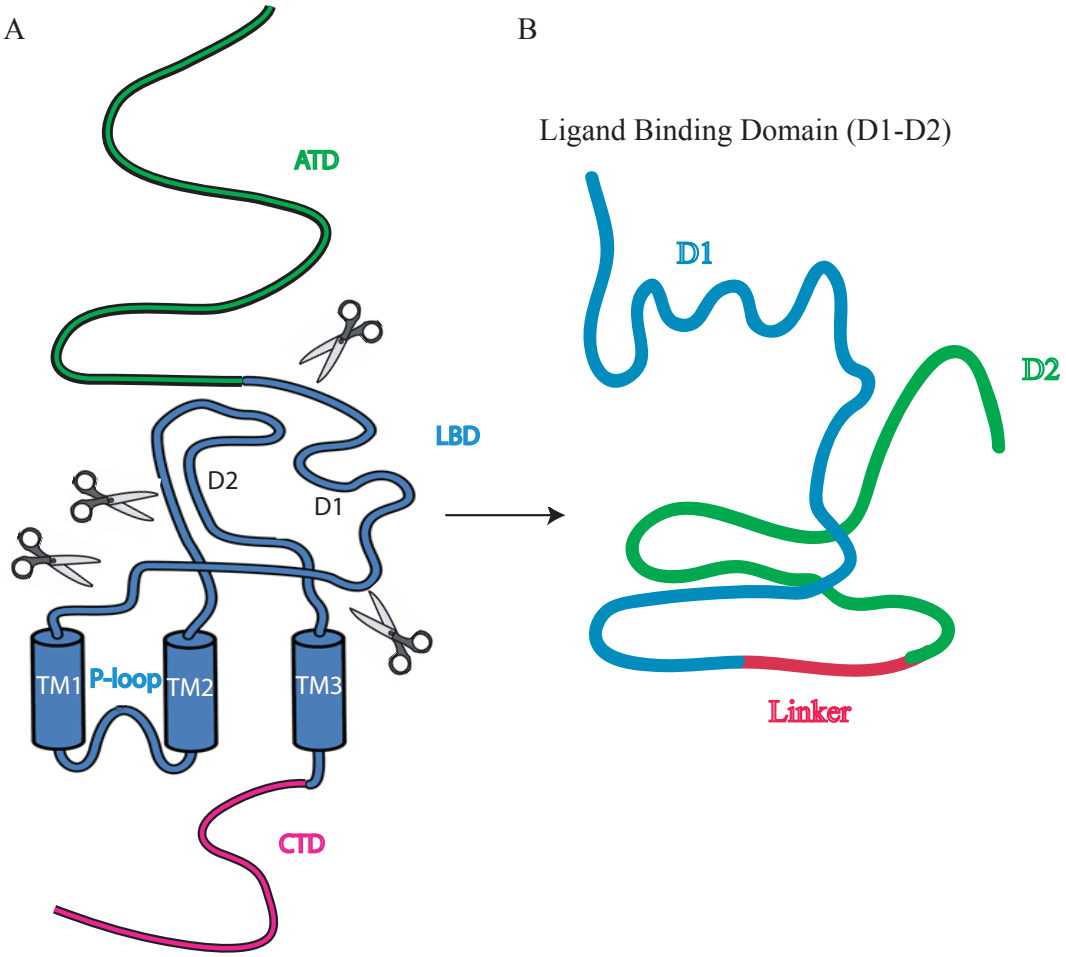

Figure 3.2 A) Topology of iGluR subunit containing an amino-terminal domain (ATD), ligand-binding domain (LBD), and three trans-membrane domains with a re-entrant P-loop followed by the carboxy-terminal domain (CTD). The scissors depict where PCR reactions were used to isolate fragments of S1 and S2 to produce a new ligand binding construct (called S1S2) used in x-ray crystallography. B) Ligand-binding domain clamshell resulting from the D1 (blue) and D2 (green) portions connected by a linker region (red).

Prior to the crystallographic studies, several key experiments suggested that the agonist-binding core consisted of two domains, similar to bacterial periplasmic proteins. The first experiment inserted N-glycosylation and proteolytic sites into the protein, digested the protein enzymatically, and analyzed the resultant fragments by gel shift to indicate domain topology (*7-10*). The second experiment used that evidence in combination with homology modeling to demonstrate that the agonist-binding domain

had structural similarity to the crystallized bacterial periplasmic proteins (*11-13*).

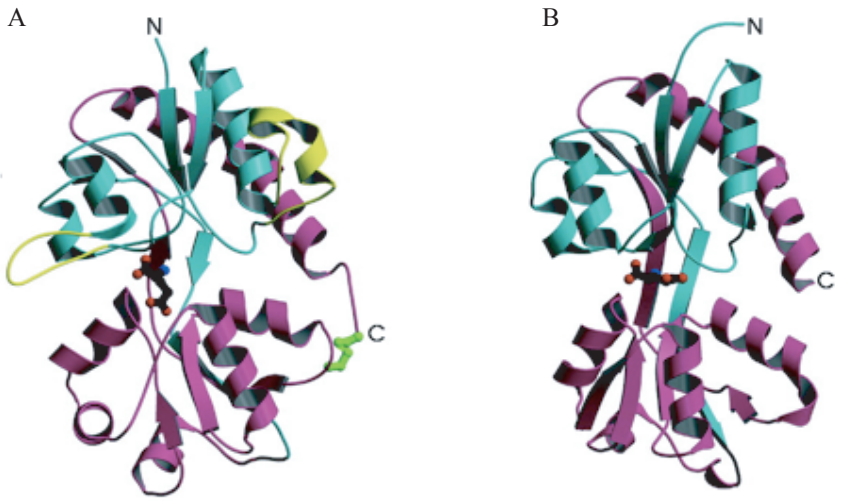

Figure 3.3 A) Topology of ligand-binding domain of GluR2 with glutamate bound in the cleft between D1 (blue) and D2 (purple). B) Topology of LBD of GluR0 with glutamate bound in cleft although in a different orientation from (A). Adapted from reference (*14*).

These studies suggested that by using protein engineering, it would be possible to isolate the ligand-binding domains. The isolated domains were water-soluble and retained the agonist binding characteristics specific for AMPA receptors. The ATD was removed, and the D1 and D2 portions of the LBD, normally separated by several of the trans-membrane domains, were hooked together with a linker (Figure 3.2). Initial studies performed in *Escherichia coli* (*E. coli)* yielded the excised soluble D1-D2 connected domains of the GluR4 AMPA receptor subtype (*15*), yet the soluble LBD was not optimized for crystallization. Continued protein engineering and use of a special *E. coli* strain, optimal for proteins containing disulfide bonds, generated high resolution structures (1.5Å) of the GluR2 AMPAR subunit in complex with the agonist kainate (*6, 16, 17*). These results spurred the isolation of other glutamate-binding cores from the bacterial GluR0 subunit, mammalian GluR4, GluR6, NR2A, and the glycine-binding NR1 subunit (Figure 3.3) (*18-21*).

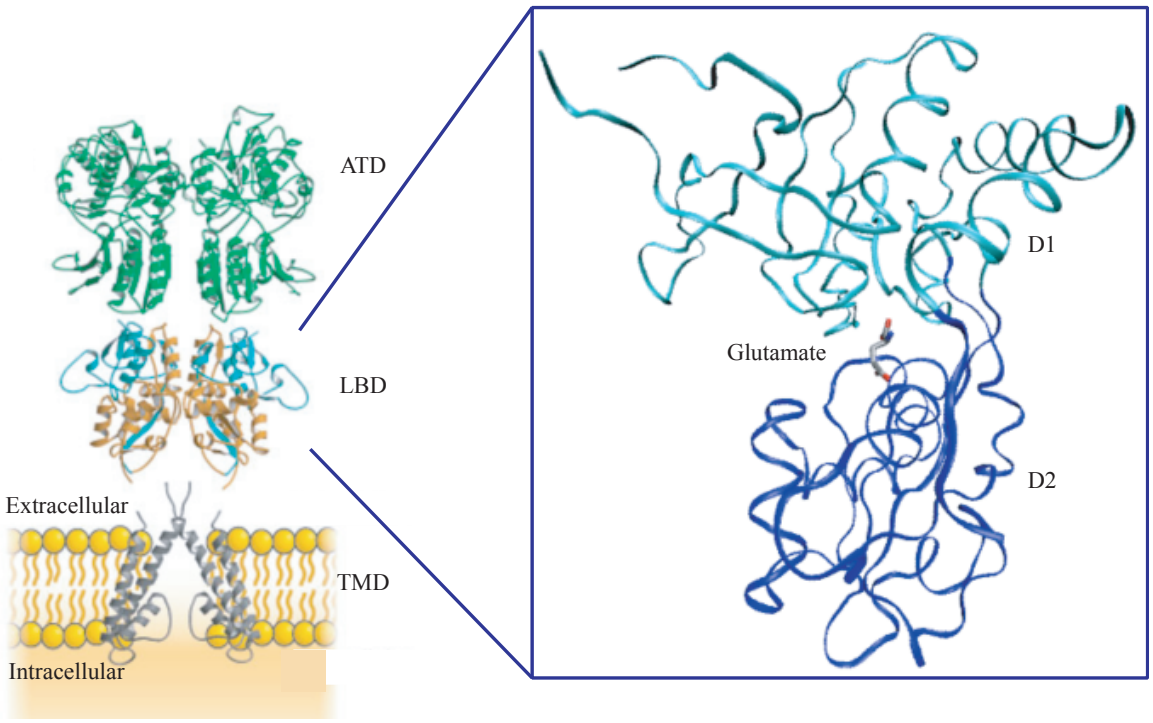

Figure 3.4 Extracellular ligand-binding domain of GluR2 AMPA receptor subunit co-crystallized with the agonist glutamate. The ligand binds to a cleft formed between D1 and D2 of the LBD. The GluR2 PDB file, 1FTJ, adapted from reference (*22*).

Not surprisingly, the results from the LBD crystal structures demonstrate a bi-lobed domain topology with D1 and D2 enclosing a cleft where the agonist binds. The D1 portion (pre-TM1) forms the top portion of the cleft and D2 (post-TM2) encloses the bottom of the cleft. The overall topology resembles a clamshell and is often referred to as such. Initial structures were crystallized in the presence of kainate(*6*), but further studies produced the clamshell in a ligand-free (apo) state and with many agonists, partial agonists, and antagonists binding in the cleft between D1 and D2 (Figure 3.4) (*18, 19, 22*). Currently, there are more than 20 structures, and all iGluR subtypes (AMPA, NMDA, and Kainate) are represented, each in complex with many different ligands. Additionally, to complement the static images of the LBD, NMR was used to obtain dynamic data on the GluR2 LBD (*23*). The first and most studied iGluR LBD is the GluR2 AMPAR subunit, which has provided the first mechanistic insights into ligand binding.

A globular protein consisting of two-domains, each representing a lobe of a

clamshell, encloses a cleft that characterizes the extracellular LBD (Figure 3.4). The two lobes are connected by two anti-parallel β-strands and are structurally similar to a periplasmic glutamine-binding protein, GlnBP (*24*). Interestingly, the domains are formed from peptide segments of both S1 and S2. The S1 segment corresponds to the peptide from the pre-M1 domain and S2 is the peptide fragment corresponding to the post-TM2/pre-TM3 segment. Both S1 and S2 contribute to D1 and D2 demonstrating that these peptides are not discreet domains within the LBD (*6*).

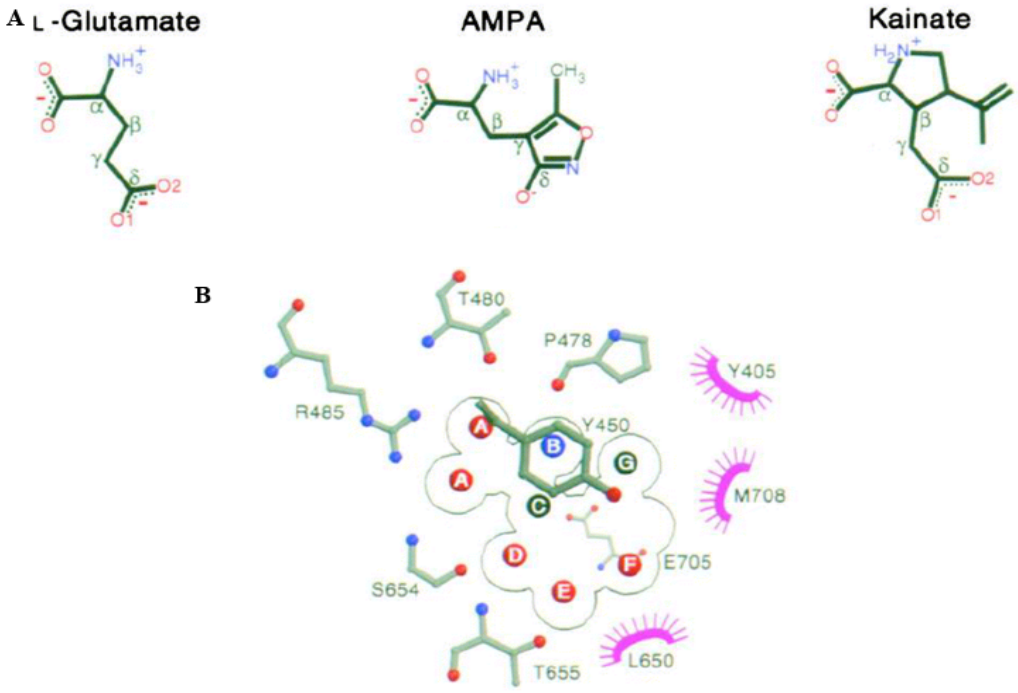

Figure 3.5 A) The agonists L-glutamate, AMPA, and Kainate with labeled carbon architecture. B) Amino acid side chains involved in ligand recognition in GluR2 subunit. The figure was adapted from reference (*22*).

Crystalization of the GluR2 LBD with the agonists glutamate and AMPA, the partial agonist, kainate, and the apo state established the specific interactions that are important for ligand activity and demonstrated that a large conformational change occurs upon ligand binding (*22, 25*). The structural evidence coupled with additional biochemical investigations (*26*) suggests a two-step process leading to channel activation. The first step, ligand docking, occurs as the ligand binds to D1 (top lobe) amino acids via

the α-amino and α-carboxy groups in the cleft between D1 and D2 (Figure 3.5A). Then the γ-carboxyl group interacts electrostatically with the base of helix F, the N-terminal dipole of which points into the cleft (Figure 3.5B). This interaction is referred to as the "locking" step and involves the movement of D2 toward D1, which closes or clamps the binding cleft (*14*). The structures with bound glutamate and AMPA demonstrated cleft closure involving a rotation of D2 towards D1 by ~21° compared to the open-cleft apo structure (*22*).

The ligand-binding domains form dimers with the S1-S2 linkers that replace the ion channel pore positioned on the same side of the dimer interface. The dimers make contact exclusively through D1, and the knowledge of this interaction combined with agonist binding that involves D2 rotation towards D1 suggested a mechanism that would open the ion channel. The dimers are connected such that each agonist binding cleft points outward from the dimer interface and upon agonist binding the closed cleft conformation is stabilized, and the linker regions of S1-S2 (on D2) swing apart from one another. As D2 moves closer to D1 to close the cleft, it pulls or twists the ion channel domain open (Figure 3.6).

The interactions that occur at the dimer interface also translate to differences between the desensitization kinetics of each ion channel. Desensitization refers to a physical state of the receptor where ligand is bound to the LBD, but the ion channel is in a non-conducting state. The interactions that contribute to ion channel gating also affect desensitization. Again, there are many structural similarities between the dimer interfaces of all the iGluR subunits, however more subtle features contribute to varying degrees of densensitization observed for each receptor. For example, most AMPARs undergo rapid desensitization whereas NMDARs experience much slower desensitization and some do not desensitize at all. Many of these features can be attributed to chemical-scale interactions at the dimer interface.

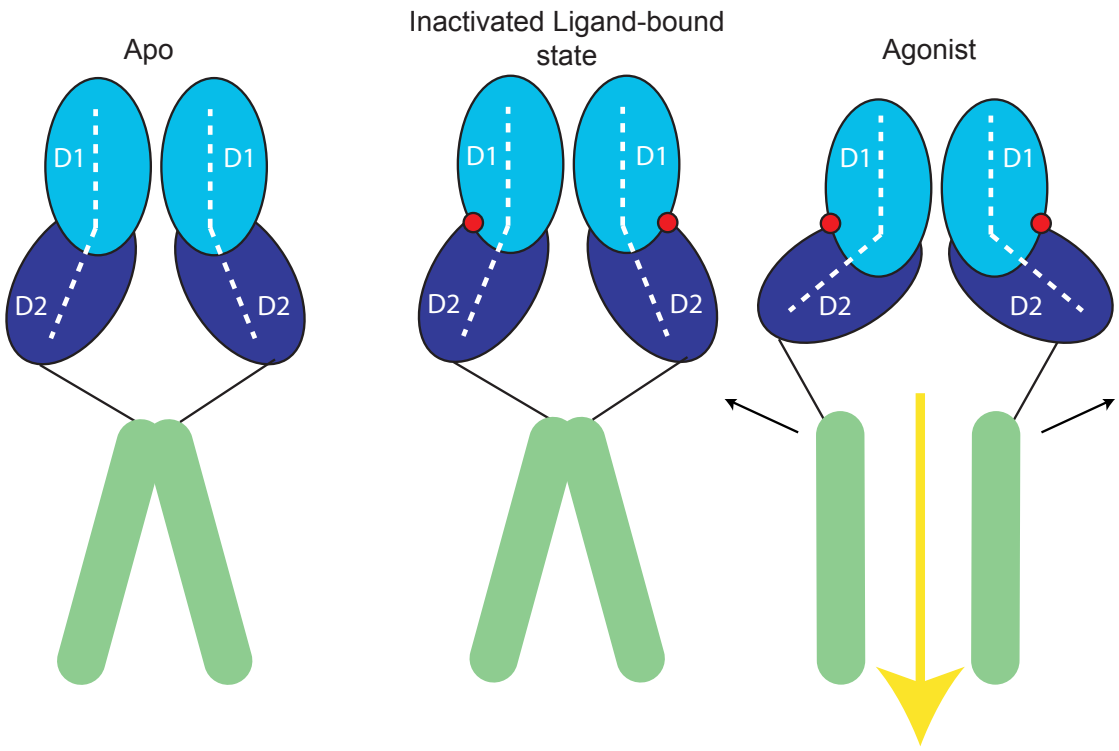

Figure 3.6 Diagram for proposed ligand-induced activation. The ligand-binding core is attached to the ion channel domain via a linker and as D2 moves toward D1, a conformational change opens the channel pore domain.

Crystallographic evidence supports the assembly of dimers for GluR2 AMPARs, the GluR0 bacterial homologue, and the NR1/NR2 NMDARs. This feature is unique since the structurally related bacterial periplasmic-binding proteins do not assemble into dimers in solution or in crystals. Additionally, the dimer interface of iGluRs is mostly hydrophobic, whereas the homologous surface of the periplasmic proteins contains many charged amino acids that do not establish complementary contacts when superimposed as a dimer (*21*). The iGluR dimer interface has evolved to support a structure that requires subtle conformational changes during ion channel activation and desensitization and remains a target for many different structural studies.

The extent to which these structural studies have expanded our knowledge of iGluR structure, activation, and function cannot be expressed enough. Although all of the iGluR families are related, the subtle features of each family do not always translate to another, so we must perform biochemical experiments for all of the different iGluRs to understand

them fully. We cannot assume that a mechanism that applies to one type of receptor will automatically apply to another, as we will demonstrate below.

Another caveat to structural studies is that although they provide precise molecular-level details, they do not assess the receptor in its native state or the full protein conformation. This is where our functional studies are key. We will use the structural evidence to guide our experiments and produce functional data for these ion channels.

3.1.2 Previous Studies of Partial Agonism and Structural Evidence for the Clamshell Model of Partial Agonism in AMPA-Selective Receptors

The methodology developed by Gouaux and co-workers is not solely applied to studying full agonists. Many studies have been performed using the S1-S2 LBD in complex with competitive antagonists and partial agonists. Competitive antagonists bind to the agonist recognition site but do not activate a receptor according to classical receptor models (*27*). Studies of AMPA-selective receptors were first performed on the GluR2 S1-S2 LBD structure, and we will summarize the observations of this receptor subtype, as they formed the basis of analysis on additional receptors. The iGluR competitive antagonists are generally larger in size than the agonists, and therefore the basic assumption is that they prevent ion channel activation via steric interference. Two GluR2 competitive antagonists, DNQX (6,7-Dinitroquinoxaline-2,3-dione) and ATPO ((*R*,*S*)-2-amino-3-[5-t-butyl-3-(phosphonomethoxy)-4-isoxazolyl]propionic acid), were crystallized with the GluR2 S1-S2 LBD and both prevent receptor activation by steric interference, a mechanism often referred to as the "foot in the door" (*22, 28*). From a chemical standpoint these antagonists are unrelated; DNQX is a quinoxalinedione and ATPO is an isoxazole (Figure 3.7). The 7-nitro group of DNQX is the likely "foot" that interacts with threonine 686 in D2. ATPO is structurally similar to AMPA and binds in a similar orientation. However, the 3-phosphono-methoxy moiety interacts with the base of helix F as the "foot" since it is a more extended structure than AMPA. The resulting domain closure is between 2.5 and 6.0°, insufficient for wild type receptor activation (compared to ~21° for AMPA and glutamate). The main conclusion from the experiments with antagonists is that they interact with pre-organized residues primarily in D1 and stabilize the open-cleft state of the clamshell, similar to the apo structure.

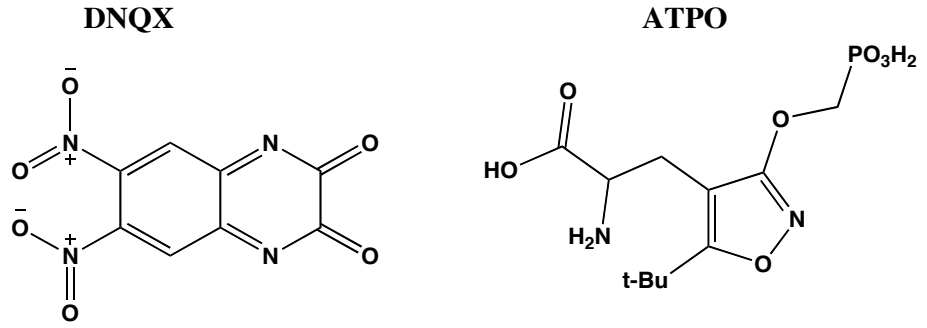

Figure 3.7 AMPA receptor antagonists, DNQX and ATPO.

The studies of GluR2 with full agonists and antagonists demonstrated a correlation between activation of the ion channel and the amount of agonist-induced cleft-closure between D1 and D2. The results with the partial agonist kainate provided more insight into the mechanism of agonist action in iGluR LBDs. Ion channel activation is characterized by at least two separate steps at the atomic level, the ligand-binding step, dependent on the receptor's affinity for the ligand, and the activation step described in terms of agonist efficacy, its ability to activate the receptor. Partial agonists are very useful molecules because they can probe the relationships among agonist binding, conformational changes of the protein, and receptor activation. Partial agonists were first described by del Castillo and Katz as ligands that have an open channel probability of less than 1 despite occupying all of the ligand-binding sites (*29*). In the absence of direct structural data, several models have been developed to explain the basis of partial agonism.

The most common method is based on the Monod-Wyman-Changeux (MWC) model for allosteric proteins (*30*). This model suggests that ligand-gated ion channels have two possible states, the closed or resting state (T) and the active or open state (R), which exist in equilibrium with each other. Agonists would shift this equilibrium in the direction of the open state. Full agonists, the most efficacious, are maximally effective at shifting the equilibrium to the open state, and partial agonists are less effective at shifting this equilibrium (*31*). This model provides a clear, but simple explanation of efficacy. However, this model may be too simple and unable to account for the ability of partial agonists to activate a spectrum of receptor efficacies (*14*).

Crystal structures demonstrating the mechanism of partial agonism in GluR2 AMPARs were solved for a variety of partial agonists. The first structures were with kainate and quisqualate, followed by willardiine (and the derivatives, 5-F-willardiine, 5-Cl-willardiine, 5-Br-willardiine, and 5-I-willardiine) (Figure 3.8), and an isoxazole series ((S)-2-Me-Tet-AMPA, (S)-ACPA, (S)-Br-HIBO) (*28, 32, 33*). One key attribute of the partial agonists is that when they bind in the closed-cleft GluR2 LBD, some of the structural water molecules that are present when glutamate is bound are excluded to support the expanded ligand structure, and some of the full and partial agonists do not bind in the same orientation as glutamate. However, this does not directly correlate with agonist efficacy. For example, AMPA and glutamate bind in a similar orientation within the cleft and are full agonists, however, the full agonists 2-Me-Tet-AMPA, quisqualate, and ACPA all bind with different orientations (*28, 33*). This suggests that the orientation of the agonist within the binding cleft is not as important for determining agonist activity as the orientation of the binding cleft itself. In other words, the receptor responds to how "full" the binding pocket is instead of how it is filled.

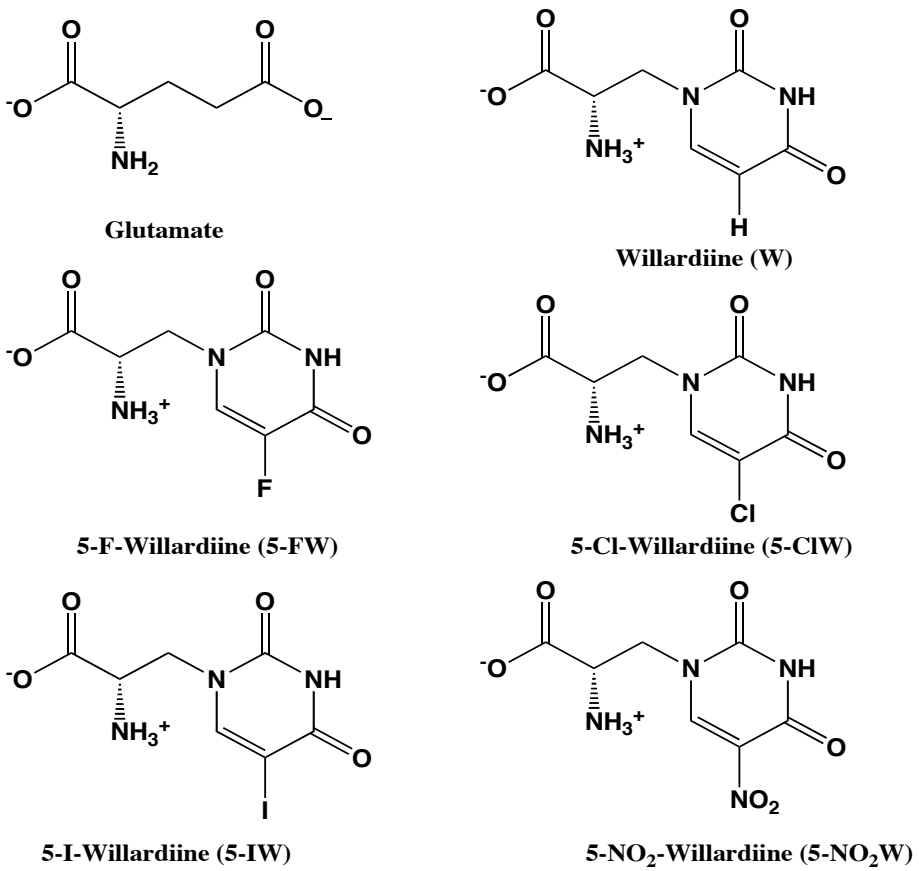

Figure 3.8 Structures of the willardiine series of GluR2 partial agonists.

The structural studies demonstrate that there is a correlation between agonist efficacy and the degree of cleft closure. The full agonists, AMPA and glutamate, induce ~20° of domain closure and kainate, a partial agonist, induces only 12° of domain closure, relative to the apo conformation. These results suggest that the amount of domain closure is related to the activity of the ion channel. Further studies with the willardiine series (Figure 3.8) were performed and acted as an ideal test case since they bind to the cleft in an orientation similar to glutamate. The willardiines act as partial agonists due to the substitution of the 5-substituent on the uracil ring, which stericly interferes with GluR2 Met708 preventing full cleft closure. The substituted willardiines, 5-H, F, Br, and I were studied (Figure 3.8) and as the size of the 5-substituent increases, the extent of activation of the ion channel diminished (i.e., agonist efficacy decreases) (*32*).

The extent of cleft closure in the GluR2 dimer was measured by evaluating the

distance between the protomer linker regions. An increase in domain closure correlates to an increase in the distance between the protomer linkers. The linkers replace the region corresponding to the ion channel pore domain of the full-length receptor; therefore an increase in the distance between the linkers suggests a physical mechanism for channel activation. To demonstrate the correlation between agonism and domain closure, plots were generated with relative agonist efficacy on the x-axis and linker separation (Å) on the y-axis (Figure 3.9) (*28, 32, 34*). One feature of these plots demonstrates a linear correlation between agonist efficacy and linker separation, consistent with the domain-closure hypothesis (Figure 3.9).

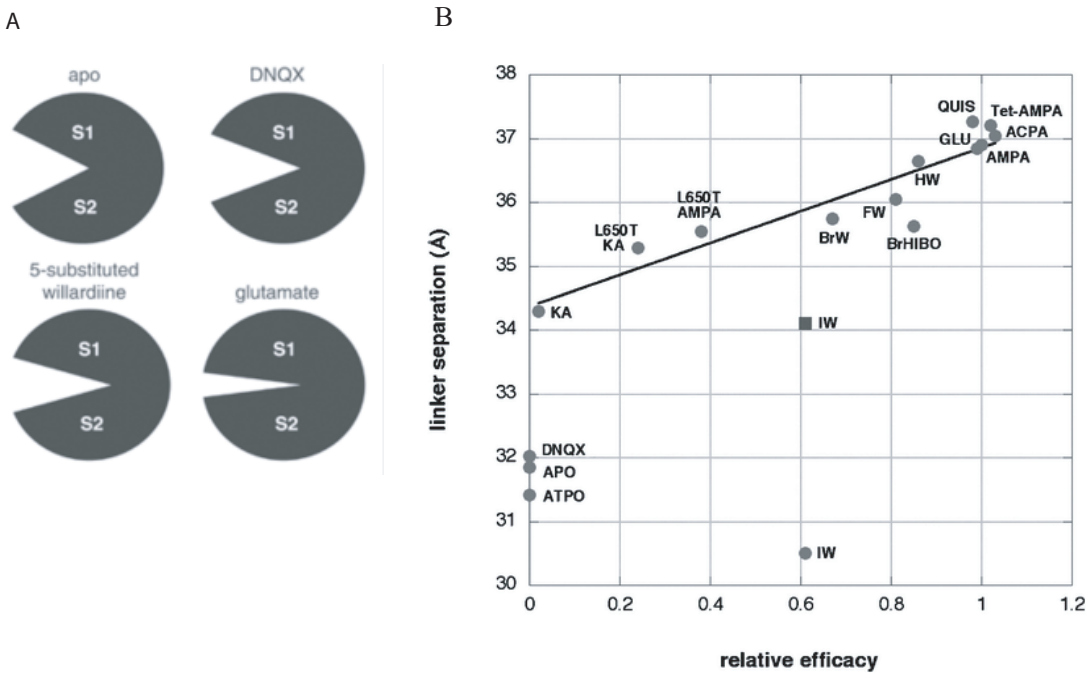

Figure 3.9 A) Schematic representing the degree of domain closure induced by full and partial agonists. Full agonists induce more domain closure relative to the apo state than partial agonists. B) Plot of the relative efficacy of different agonists vs. the distance of linker separation measured from the GluR2 S1-S2 crystal structures (Å). Adapted from references (*28, 32, 34*).

Single-channel analysis of full-length ion channels suggests how structural changes in the binding core couple to ion channel activation. Several conductance states have been identified for iGluRs, some conducting more than others. Conductance states are

open-state conformations of the ion channel defined by a particular ion flux. iGluR partial agonists preferentially activate lower conductance states, and full agonists activate higher conductance states. The existence of multiple conducting states for the ion channel suggests that the degrees of domain closure exist along a continuum. More importantly, it suggests that the conformational changes signaled to the ion channel domain by the ligand binding domain exist as specific states along this continuum. In other words, the degree of ligand binding domain closure promotes population of specific conductance states (*32*) presumably that coincide with specific amount of ion channel opening (Figure 3.10). Another study supporting this idea involved mutation of GluR2 Leu650 to Thr. The L650T mutation decreased AMPA efficacy without a change in domain closure, but kainate efficacy increased, becoming a full agonist with an increase in domain closure (*25*). These studies imply that agonists induce ion channel activation via several mechanisms. However, further investigation of the structure and function of iGluRs with partial agonists are necessary for a better, more complete understanding of these mechanisms.

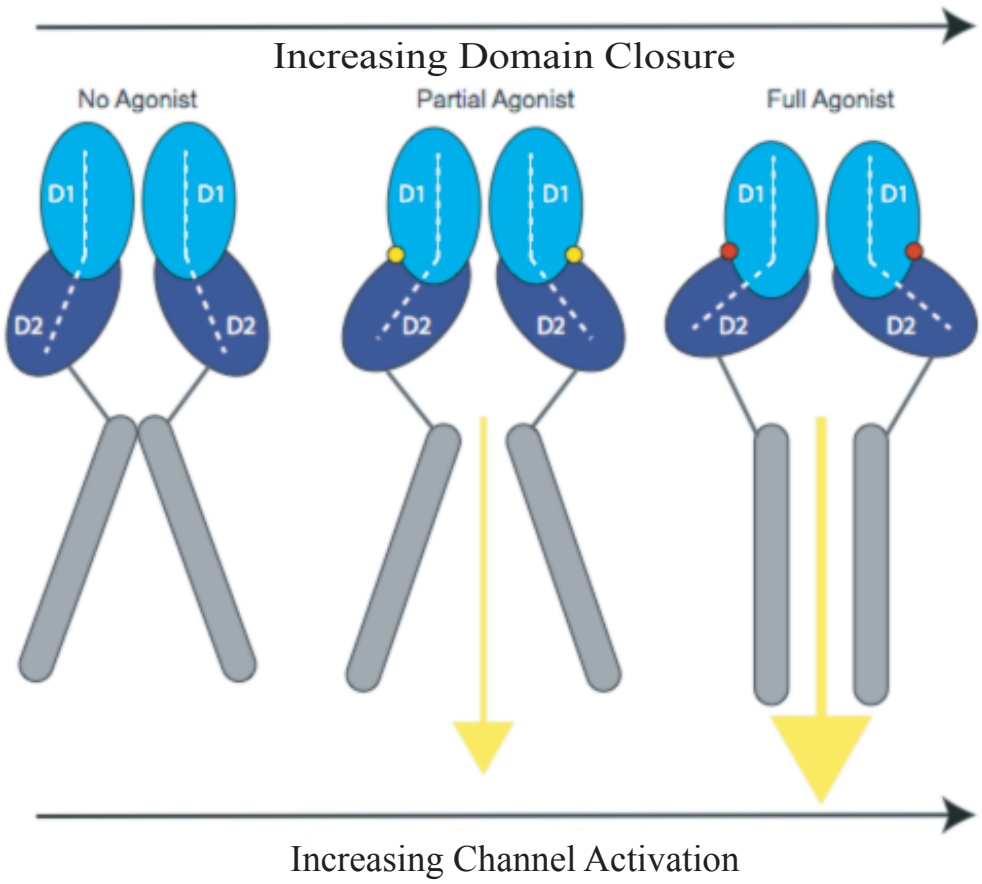

Figure 3.10 Schematic representing the partial ion channel opening induced by partial agonists and a larger channel opening induced by full agonists.

3.1.3 Structural Studies of NMDA-Selective Receptors

NMDA receptors are unique in the glutamate family of ion channels for many reasons, but they are especially peculiar in terms of ligand binding, since the endogenous ligand for the NR1 subunit (a requirement for channel function) is glycine or D-serine, not glutamate (*1*). The first structural understanding of NMDA receptors came from crystal structures of the S1-S2 region of the NR1 glycine-binding domain (*18*). Gouaux and coworkers demonstrated that similar to bacterial periplasmic proteins, bacterial GluR0, and mammalian GluR2 and GluR6, the NR1 LBD folds into a D1-D2 clamshell. Several years after these structures were solved, the soluble S1-S2 NR1-NR2A heterodimer was characterized (*19*) in the presence of glutamate and glycine (Figure 3.11). These studies and biochemical studies, with disulfide crosslinked NR1-NR2 receptors, demonstrated that the native NMDAR forms a dimer of heterodimers instead

of a composite of NR1 homodimers and NR2 homodimers (*19*). Uniquely, NMDA receptor dimer assemblies involve allosteric coupling between the two different subunits. The heterodimer suggests that unlike the AMPAR LBD dimers, the NMDAR dimer interface consists of both D1 and D2 contacts. This could be one contributing factor affecting the differences observed among NMDA receptor assemblies (*35, 36*).

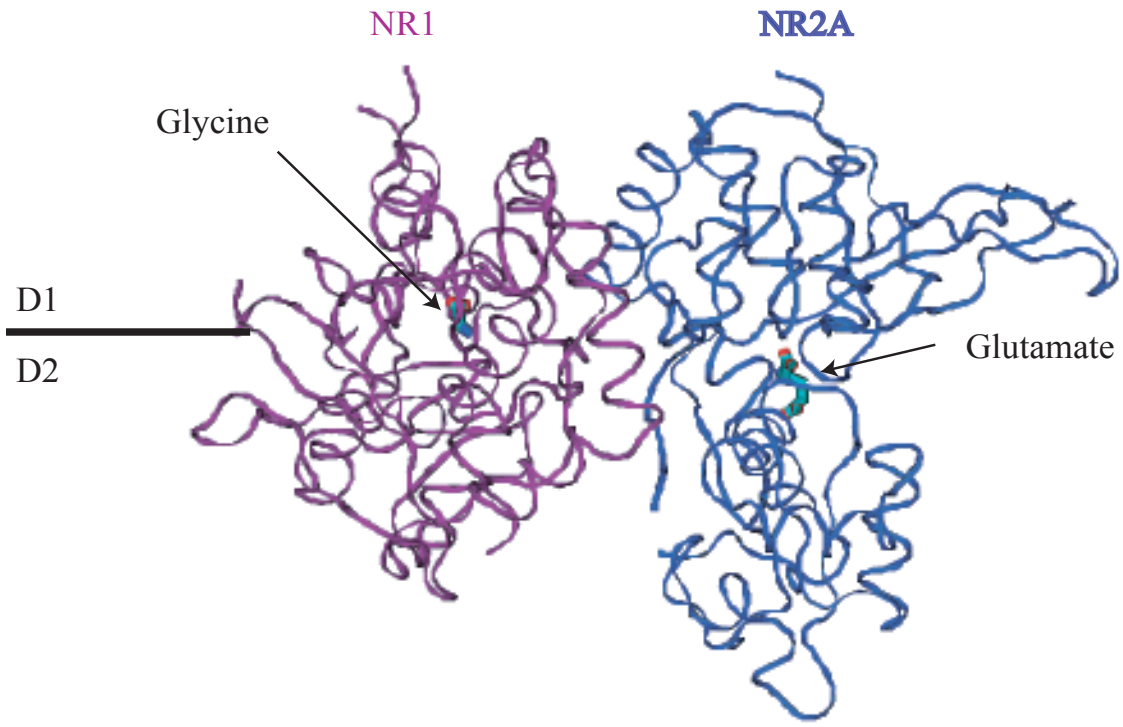

Figure 3.11. NR1-NR2A heterodimer structure. Glycine is bound to the NR1 subunit and glutamate is bound to the NR2A subunit. The dimer interface is composed of both D1 and D2 contacts. PDB file: 2A5T (*19*).

The NMDAR glutamate and glycine agonist-binding domains share several characteristics with the GluR S1-S2 structures, including conserved residues that appear in all of the iGluR families. An arginine in Helix D forms the major binding site for the α-carboxyl group of the ligand. Helix F contains a conserved threonine or serine, which makes a hydrogen-bond contact with the γ-carboxyl group (e.g., in NMDARs it contacts the main-chain peptide bond). The α-amino group makes contact with a conserved glutamate residue in AMPA and KA receptors, and in NMDA receptors it makes a

solvent-mediated contact with an aspartate residue (Figure 3.12).

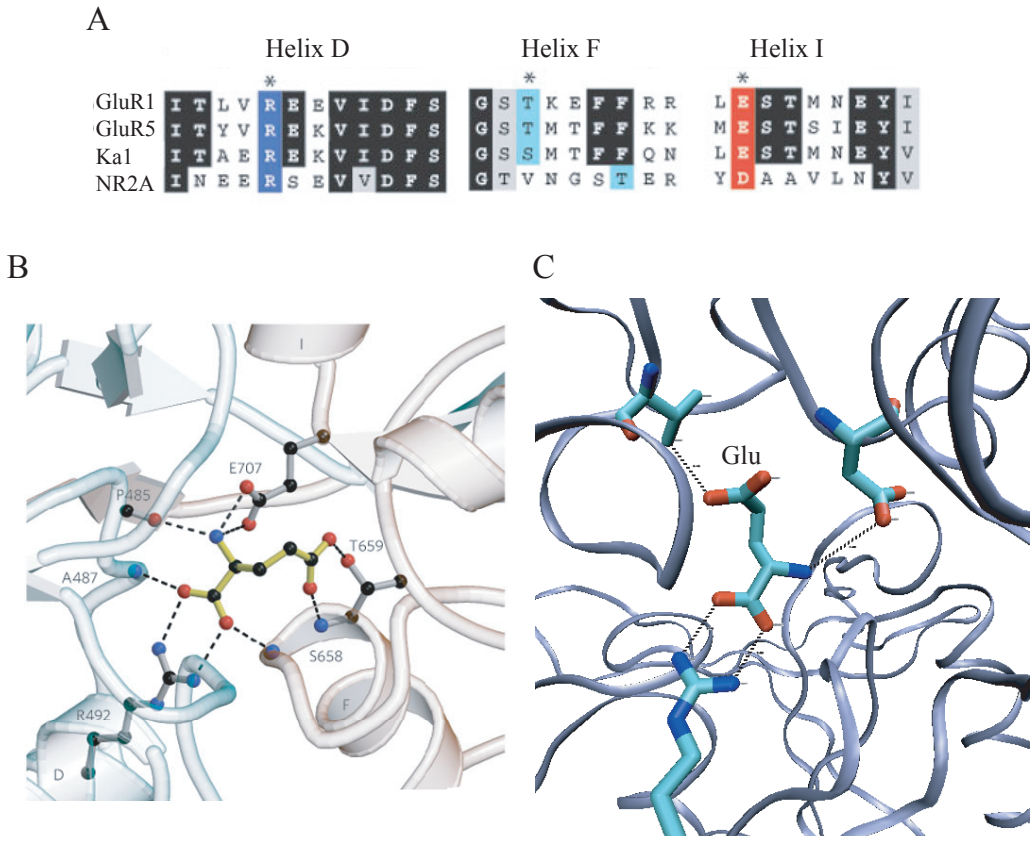

Figure 3.12 A) Sequence alignment of helices D, F, and I, which are involved in ligand binding. B) Conserved structural contacts between helices and glutamate (GluR6 S1-S2 domain), adapted from reference (*37*). C) NR2A binding site with conserved residues highlighted, PDB file 2A5T.

These structures demonstrate that in all of the binding pockets there is more than enough room to accommodate glutamate and related structures with the exception of NR1, which is just large enough to accommodate glycine and excludes the larger glutamate residue (*18*). The D2 portion of the clamshell provides subunit specificity for different ligands. In all iGluRs, D1 has conserved structure and binding interactions with the α-carboxyl and α-amino groups from the ligands. The most important theme, which we will revisit in our studies, is that the amount of agonist-induced domain/clamshell closure varies between each of the receptor subtypes, as well as for individual agonists, antagonists, and partial agonists (*18, 20, 22, 27, 28, 38*).

3.1.4 Previous Studies of Partial Agonism and the Clamshell Model of Partial Agonism in NMDA Receptors: The NR1 Glycine-Binding Subunit

Partial agonism studies were performed on the NR1 S1-S2 LBD prior to the characterization of the heterodimer complex. These studies paralleled those of GluR2, but with NR1 specific partial agonists, 1-aminocyclopropane-1-carboxylic acid (ACPC), 1-aminocyclobutane-1-carboxylic acid (ACBC), and D-cycloserine (D-CS) (Figure 3.13) and the antagonist, cycloleucine. The first study demonstrated that the partial agonist, D-CS, induced similar domain closure to glycine, an unexpected result based on the previous partial agonist studies with GluR subunits (*18*). This study prompted a more thorough investigation of NR1 partial agonism using additional partial agonists and antagonists.

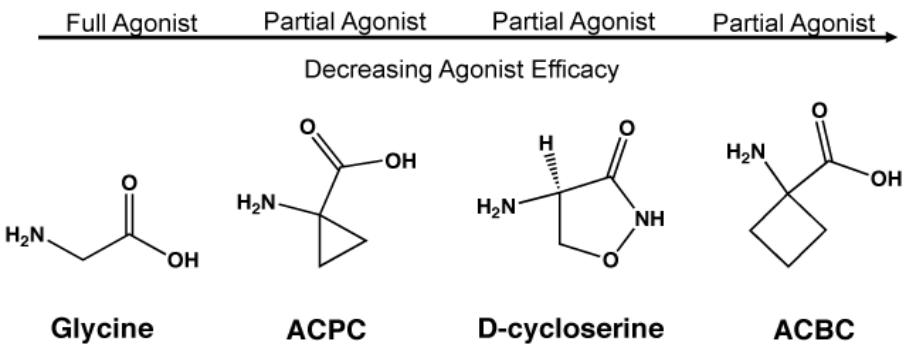

Figure 3.13 Chemical structures of NR1 ligand-binding domain partial agonists.

The study used these different partial agonists, which increase in volume by ~11 $Å^3$ per molecule (*18*). The conclusion of the study was that the NR1 S1-S2 core behaves differently than the AMPA-sensitive ligand-binding core in the presence of partial agonists. The NR1 glycine-selective subunit ligand-binding domain undergoes the same degree of clamshell closure for partial agonists as it does for full agonists (*39*) (Figure 3.14). Previously established models depicting the interactions between ligand-binding domain conformational states and how they translate to ion channel activity are complicated by these results (*32*). Full agonists for AMPA-selective receptors appear to shift the equilibrium towards the open state, with partial agonists stabilizing intermediate states, but the NR1 partial agonists do not fit this model. An alternative model for ion

channel activation is a two-state model in which both the ligand-binding domain and the pore domain have two states, either closed or open. Full agonists are more effective at populating an agonist-bound, open channel state than partial agonists, which are not as effective at shifting the equilibrium constant (K_{eq}) from the agonist-bound, closed channel state to the agonist-bound, open channel state (*31*). The second model can account for the observations in the NR1 partial agonist bound LBD structures, but differs from the mechanism thought to occur in GluR2 receptors (Figure 12).

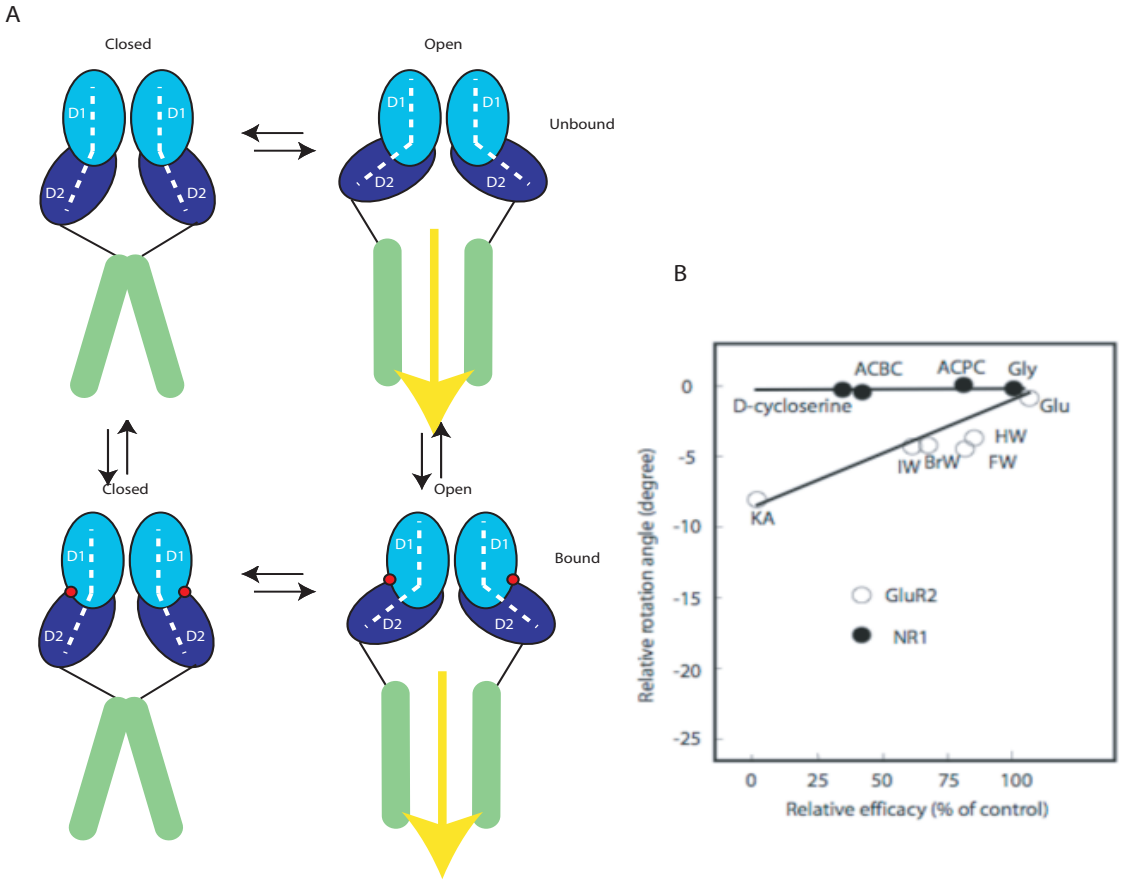

Figure 3.14 A) Scheme of model depicting NR1 agonist efficacy and channel activation. B) Graph of relative agonist efficacy versus S1-S2 domain closure for NR1 and GluR2 receptors. No correlation is observed for NR1 compared to the GluR2 subunit**,** adapted from reference (*31*).

To understand the binding of partial agonist to NR1, Gouaux and co-workers analyzed the contacts between D1-D2 and the agonists. All of the agonists- glycine, ACPC, and ACBC- interact with a similar hydrogen bond scheme among the domains

and the carboxy and amino groups. A hydrophobic surface of the LBD (Phe484, Val689, and Trp731) interacts with the rest of the hydrophobic portion of the ligands and since it is primarily composed of D2 residues, it is possible that these residues "sense" the size of the ligand and undergo localized conformational changes in the clamshell that translate to receptor activation (*39*). D-CS interacts similarly to glycine with a couple of subtle differences. The nitrogen and exocyclic oxygen interact with Arg523 similarly to the glycine α–carboxylate of glycine. The isoxazolidinone ring oxygen interacts with Ser688 instead of the α–carboxylate oxygen (in glycine structure) (*18*). NR1 Val689 is implicated in changing the conformation of helix F and the inter-domain β strand, believed to be implicated in receptor activation. It is possible that NR1 compensates for increasing the ligand size, using a different mechanism than glutamate-gated subunits (*40*). Since the amount of clamshell closure is not as important for NR1 subunits, this suggests that the other regions of the protein (possibly the dimer interface) are more important for translating conformational changes induced upon agonist binding. The conclusion from the structural studies is that even though NR1 partial agonists induce the same domain closure as full agonists, they do not stabilize the closed-clamshell as well as full agonists, as evidenced by their efficacy.

3.1.5 Previous Studies of Partial Agonism and the Clamshell Model of Partial Agonism in NMDA Receptors: The NR2 Glutamate-Binding Subunit

The S1-S2 heterodimer containing both NR1 and NR2A subunits is the only current structural characterization of any NR2 subunits. Crystal structures of the NR2 agonist-binding clamshell with partial agonist bound remain elusive. However, there has been a plethora of biochemical and *in silico* studies performed on NR2 subunits. As mentioned above, residues that interact directly with the ligands across all iGluRs are highly conserved, and an increase in solvent-mediated interactions distinguishes the NR2 agonist binding cleft. The α-amino group of glutamate interacts with NR2A Asp712 (mature protein numbering) through a water-mediated interaction.

In addition, several hydrogen bonds have been identified between D1 and D2 residues that are thought to contribute to agonist-induced activation of the ion channel. The Asp (712) residue also makes an inter-domain interaction with Tyr742. Another D2

residue, Tyr711 (NR2A mature protein numbering), interacts with a D1 residue, Glu394, as well as the γ-carboxylate of the ligand (*34, 41*) (Figure 3.15). Mutagenesis studies were performed on several of these residues, most notably a mutation in NR2B, Tyr705Ala (NR2AY711 equivalent), which resulted in a >400-fold shift in glutamate EC_{50} (*42*). Additional kinetic experiments also demonstrated that this residue was important for receptor activation, possibly through inter-domain interactions. These studies provide clear evidence that although crystal structures are useful for understanding the nature of chemical-scale interactions, without full-length, functional ion channels we cannot get a clear understanding of how structure relates to function, and thus it is important to correlate mutagenesis with structural studies.

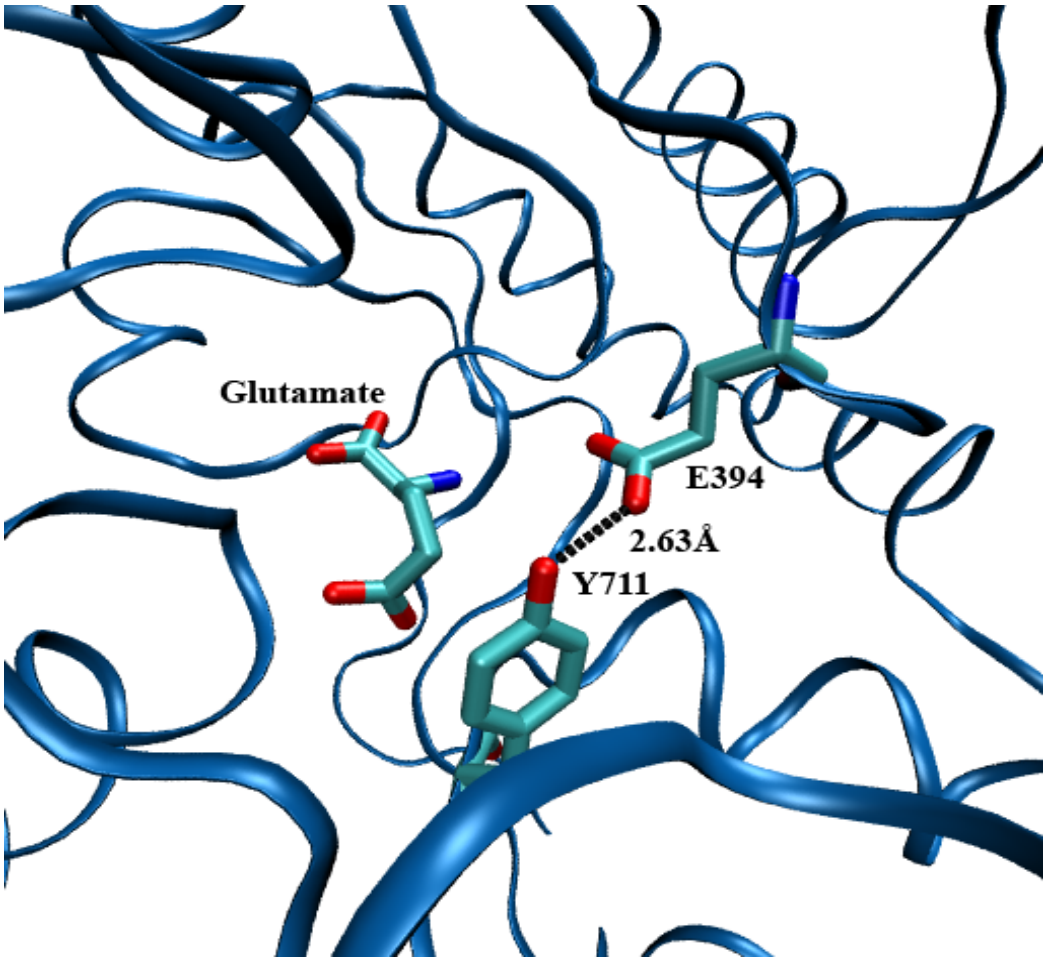

Figure 3.15 Ligand-binding domain of the NR2A subunit (PDB file 2A5T). The ligand, glutamate, is highlighted and an inter-domain hydrogen bond between E394 (D1 residue) and Y711 (D2 residue) is labeled.

3.2 NMDA Receptor Ligand-Binding Domain Studies

3.2.1 Project Overview

To further explore the relationship between structure and function, we decided to incorporate unnatural amino acids into the ligand-binding site of the NR2B glutamate-binding subunit of the NMDA receptors. We hypothesized that amino acids that lie at the agonist-cleft interface could interact with the agonist and induce ion channel activation. Since previous studies had implicated NR2BY705 (NR2AY711, Figure 3.15) in an ion-pair interaction with NR2BE387 (NR2AE394, Figure 3.15), we decided to begin our studies with these residues (all numbering will be for the mature protein). In particular, we sought an alternative probe of the clamshell mechanism, one based on receptor *function*, rather than a series of structures of receptor fragments. Along with complementing the structural work, such an approach could be more generally applicable to a wide range of receptors. Our focus is on residues at the D1-D2 interface that have been implicated to be important in receptor function, and that, based on the structural studies, appear to be in a critical position with regard to clamshell closure. Using unnatural amino acid mutagenesis, we have influenced clamshell closure by inserting a "stick" in the clam to prop it open, and we then evaluated the impact on activation of the receptor by agonists and partial agonists.

3.2.2 Studies of an Ion-Pair Interaction at the NR2B D1-D2 Interface

To examine the inter-domain interactions, we utilized nonsense suppression to incorporate Tyr, Phe, 4-Me-Phe, and 4-MeO-Phe at NR2BY705 (Figure 3.16). We analyzed full-length functional receptors to measure whole-cell currents and determine EC_{50} values and relative efficacies for each of the mutant receptors. Relative efficacies were determined by measuring the I_{max} partial agonist/I_{max} L-glutamate. Also, responses to all of the NR2B agonists were measured in the presence of 10μM glycine. As mentioned above, a previous study indicated that the conventional mutation, NR2BY705A, resulted in >400-fold shift in L-glutamate EC_{50} (*42*). This result is not surprising since the alanine mutation completely obliterates the side chain, a non-subtle mutation eliminating a hydrogen bond donor and acceptor and aromaticity.

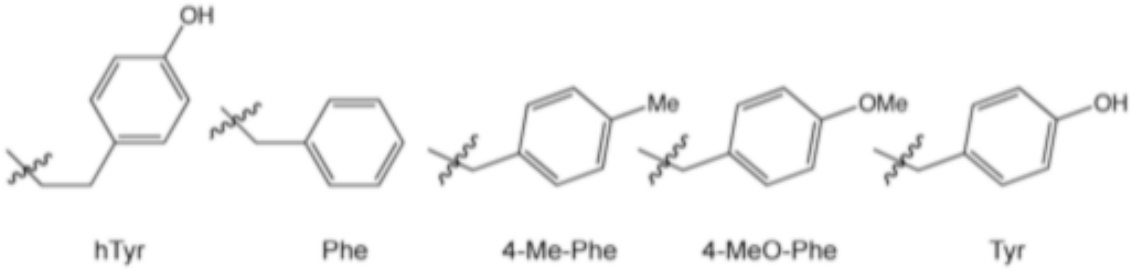

Figure 3.16 Conventional and unnatural amino acid side chain analogs of Tyr, homo-tyrosine (hTyr), phenylalanine (Phe), 4-methyl-phenylalanine (4-Me-Phe), and 4-methoxy-phenylalanine (4-MeO-Phe).

The more subtle mutations Phe, 4-Me-Phe, and 4-MeO-Phe produced functional receptors with manageable EC_{50} shifts of 14-, 10-, and 9-fold for glutamate and 23-, 9-, and 15-fold for NMDA respectively (Table 1). Overall, there are no significant differences among these mutations. All mutations remove the hydrogen bond donating ability of Tyr, but 4-MeO-Phe retains the hydrogen bond accepting ability. Our results thus suggest that an important role of Y705 is to donate a hydrogen bond. Additionally, each of these mutations produces a significant decrease in efficacy for NMDA with respect to glutamate (Figure 3.17A). Compared to wild type, where NMDA shows an efficacy of 0.88, the relative efficacies for the Phe, 4-Me-Phe, and 4-MeO-Phe mutants drop to 0.14, 0.37, and 0.26, respectively (Table 1). The drops in efficacy suggest that the hydrogen bond donating ability of Y705 is important for gating interactions that stabilize the closed, ligand-bound conformation of the clamshell. The efficacy studies also suggest that the Y705 hydrogen-bond donor is more important for stabilizing the partial agonist, NMDA, compared to glutamate, although the presence of electron density at the 4-position is important for function, even if there are no hydrogen bond donors or acceptors, as evidenced by the relative efficacy with 4-Me-Phe (Table 3.1).

Table 3.1 EC_{50} and relative efficacy for NR2B D1-D2 interface mutations with L-glutamate and NMDA (N.E. is no expression). NMDA relative efficacy is compared to L-glutamate, (S.E.M.= standard error measurement).

Receptor	Glutamate **EC_{50} μM ± S.E.M. (n)**	Glu **Hill**	NMDA **EC_{50} μM ± S.E.M. (n)**	NMDA **Hill**	NMDA **Efficacy**
wildtype (1a/2B)	2.6 ± 0.6 (8)	1.2	20 ± 1.3 (15)	1.6	0.88±0.009
1a/2BY705 Phe	36 ± 1.3 (6)	2.0	460 ± 52 (5)	2.1	0.14±0.01
1a/2BY705 4-MePhe	27 ± 2.3 (12)	1.5	190 ± 23 (5)	2.0	0.37±0.01
1a/2BY705 4-MeOPhe	24 ± 1.1 (7)	1.4	310 ± 24 (6)	1.2	0.26±0.01
1a/2BY705 hTyr	43 ± 2.4 (5)	1.5	31 ± 2.6 (7)	1.5	0.79±0.01
1a/2BE387D	50 ± 0.9 (5)	2.4	490 ±110 (6)	1.4	0.29 ±0.05
1a/2BE387Nha	92 ± 8.2 (10)	1.8	220 ± 21 (10)	1.9	0.39±0.02
1a/2BE413DY705 hTyr	N.E.		N.E.		

E387 is the proposed D1 partner of Y705. Mutation of the glutamate side chain to alanine was detrimental, producing a >200-fold shift in EC_{50} (*42*). We again sought a more insightful evaluation of the importance of the glutamate side chain, using more subtle mutations. We introduced Asp, which contains the same charge as Glu but a shorter side chain. This subtle mutation significantly affected EC_{50}, raising it by ~20-fold for both glutamate and NMDA. We next introduced the unnatural amino acid nitrohomoalanine (Nha) (Figure 3.17B). Nha acts as an isosteric and isoelectronic analogue of a Glu, but it lacks the negative charge and is also a significantly weaker hydrogen-bond acceptor (*43*). Large increases in EC_{50} were again seen, but in this case the effect was more than 3-times larger for glutamate than for NMDA. This suggests that E387 may play an important role in distinguishing different agonists.

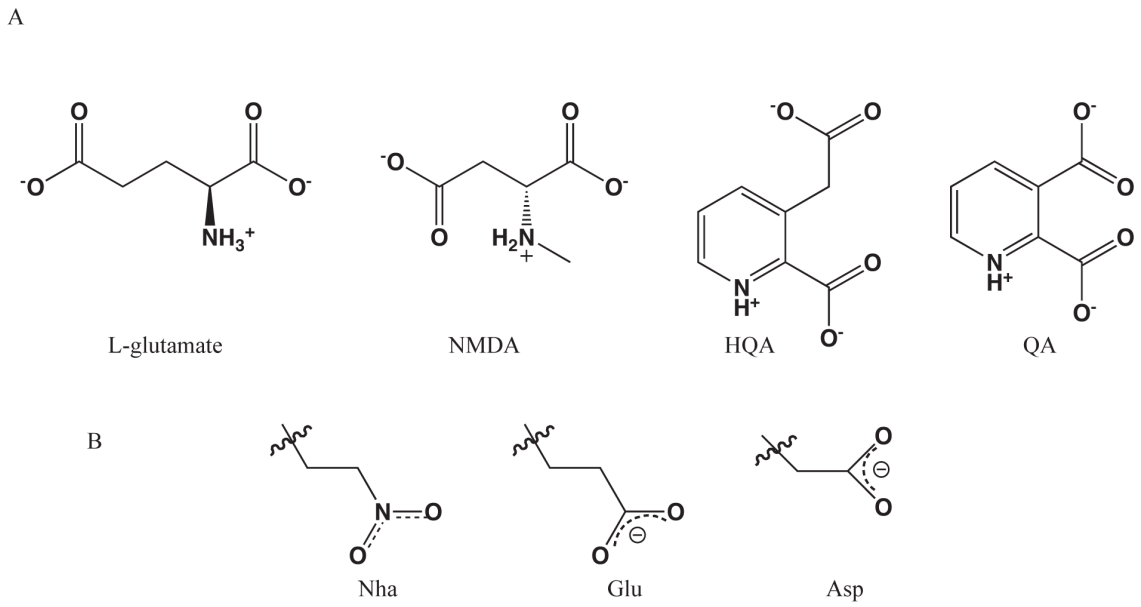

Figure 3.17 A) NR2B full and partial agonists used to study receptor function, L-glutamate, NMDA, homoquinolinic acid (HQA), and quinolinic acid (QA). B) Analogs of glutamate (Glu), aspartate (Asp), and nitrohomoalanine (Nha).

As with mutations at Y705, a drop in relative efficacy was observed for NMDA with each glutamate mutation. The effects were similar to those seen at the tyrosine, with NMDA efficacies relative to glutamate dropping to 0.29 for E387D and 0.39 for E387Nha (Table 3.1) (Figure 3.17B). All of the mutations result in a drop in relative efficacy for NMDA, suggesting that the inter-domain hydrogen bond between E387 and Y705 is directly involved in conferring changes induced by agonist binding to ion channel activation.

It has been proposed that E387 interacts electrostatically with the amino group of glutamate (*41*). The stereochemical difference between L-glutamate and NMDA suggests caution in directly comparing their binding behaviors, but the comparable responses of the two agonists to the E387D mutation suggests that the ammonium groups may be similarly positioned. Another difference between the two agonists concerns the nature of the positive charge on the agonist. The added methyl group of NMDA creates a more diffuse positive charge that spreads onto the N^{+}-methyl hydrogens (*34, 44, 45*). In contrast, L-glutamate has a more localized charge, focused primarily on its ammonium

group. The more focused positive charge on glutamate should experience a stronger electrostatic interaction with a nearby negative charge, and hence the Nha mutation is more deleterious for glutamate. We propose that both agonists experience an electrostatic interaction with E387. The penalty for the E387D mutation primarily reflects the adjustments to protein structure and/or agonist orientation in response to shortening the side chain, and both agonists are penalized to the same degree. However, with Nha, for which no such adjustment is required, the larger penalty for glutamate indicates that the intrinsic electrostatic interaction to E387 is larger for glutamate. This is consistent with expectations based on the differing electrostatics for the higher charge density of the R-NH_3^+ of glutamate compared to the lower charge density of the R-$N(CH_3)H_2^+$ of NMDA.

3.2.3 Homo-tyrosine Incorporation at Y705

Having confirmed that Y705 and E387 are important for receptor function, we wished to use them as a probe of the clamshell motion. The simple idea was to increase the size of one of the residues by introducing the one-carbon homologue, in this case homotyrosine (hTyr, Figure 3.16). This would be like inserting a stick in the clamshell, preventing full cleft closure. We anticipated that full agonists would be more strongly influenced by the stick than partial agonists, because the latter do not induce full clamshell closure according to the GluR2-based structural model. Having established that the hydroxyl group of Y705 is essential for proper receptor function, it is clear that hTyr is a superior choice to other possible bulky residues, highlighting the value of the unnatural amino acid methodology. In fact, this is the only method that could test our hypothesis without making a less subtle mutation.

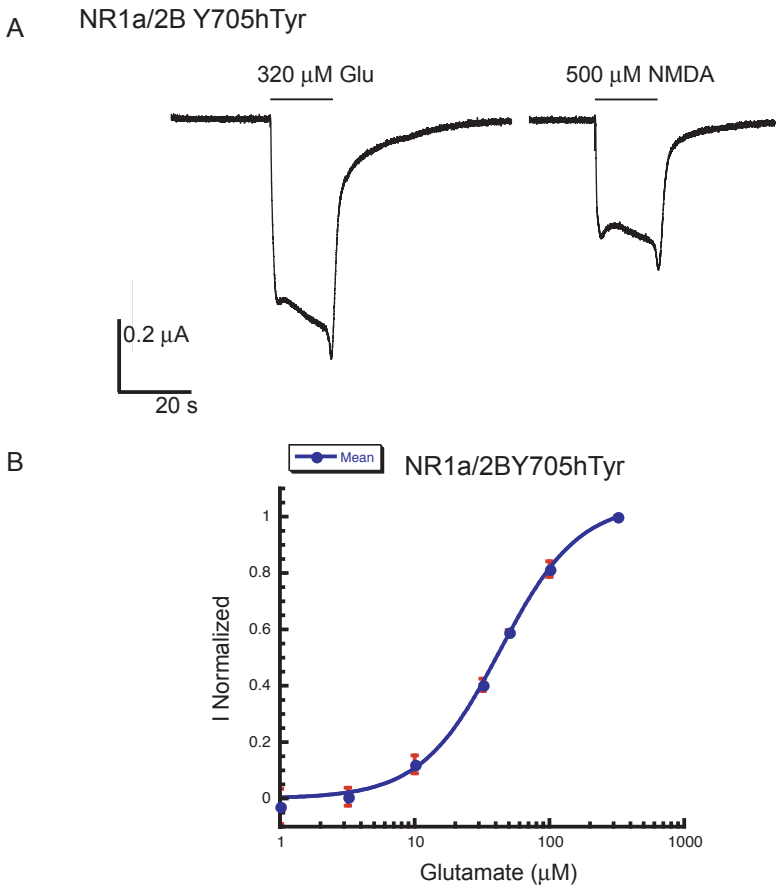

Figure 3.18 A) Electrophysiology traces of the NR1a/NR2BY705hTyr receptor. The currents were induced by glutamate and NMDA doses, as labeled. B) Example dose-response relationship for the NR1a/NR2BY705hTyr receptor and glutamate.

Initially, we measured EC_{50} values for the Y705hTyr mutant with glutamate and NMDA (Fig. 3.18). The respective EC_{50}s were shifted 16- and 1.5-fold, respectively (Table 3.1), the largest distinction between the two agonists we have seen and a result much different from the other Tyr mutants we evaluated. We considered the possibility that the new side chain geometry was affecting D1-D2 clamshell closure and that partial agonists would respond depending on their relative efficacy.

Table 3.2 EC_{50} and relative efficacy for NR2B D1-D2 interface mutations with homoquinolinic acid (HQA) and quinolinic acid (QA). HQA and QA relative efficacies are compared to L-glutamate.

	HQA			QA		
Receptor	**EC_{50} μM ± S.E.M. (n)**	**Hill**	**Efficacy**	**EC_{50} μM ± S.E.M. (n)**	**Hill**	**Efficacy**
wildtype (1a/2B)	8.1 ± 1.0 (16)	2.2	0.96± 0.002	650 ± 90 (7)	1.9	0.86±0.005
1a/2BY705 hTyr	49± 4.3 (11)	2.1	0.83±0.008	720 ± 90 (5)	2.4	0.32± 0.009
1a/2BE387D	69± 2.3 (16)	2.3	0.77 ± 0.02	690 ± 120 (10)	2.0	0.02±0.003
1a/2BE387Nha	85± 6.1 (11)	1.8	0.86± 0.006			

To further investigate the effect of Y705hTyr, we studied two additional partial agonists, homoquinolinic acid and quinolinic acid (Fig. 3.17A), with relative efficacies in the wild type receptor of 0.96 and 0.86 compared to glutamate. In response to homoquinolinic acid, Y705hTyr produced a 6-fold shift in EC_{50}, while the Y705hTyr mutation essentially did not affect the EC_{50} of quinolinic acid (Table 3.2). A trend was observed: increased efficacy of the agonist in the wild type receptor correlated with a larger shift in EC_{50} in response to the Y705hTyr mutant. These results produced a compelling relationship between agonist efficacy and receptor response (Figure 3.19). The plot is similar to ones produced for other iGluR systems, except now the y-axis is a measure of receptor *function*, rather than a structural parameter.

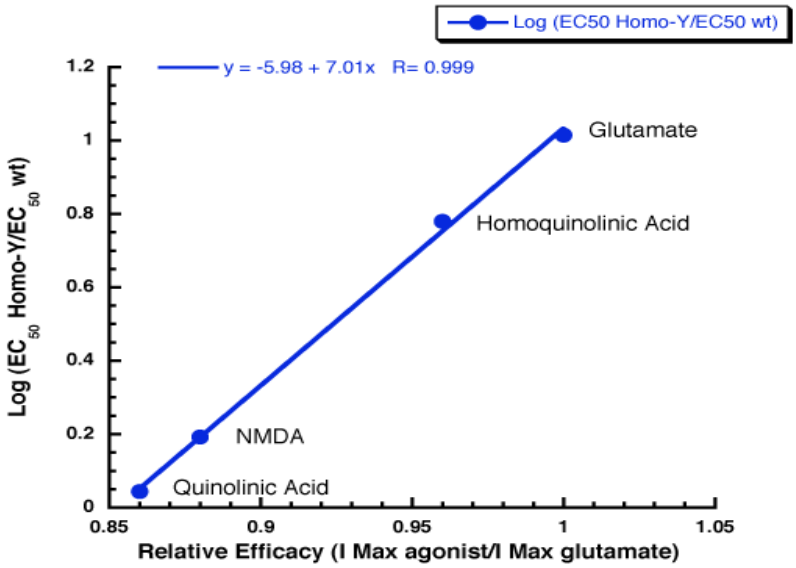

Figure 3.19 Activity of partial agonists at the NR1a/NR2BY705hTyr receptor compared to each agonists relative efficacy. A linear relationship is observed between receptor function and agonist activity. Partial agonists are less affected by the mutation than full agonists.

Since E413 and Y705 are proposed to interact directly through a hydrogen bond, we investigated whether the increased side chain length of the Y705hTyr mutation could be compensated for by the comparably decreased chain length of the E413D mutation. The double mutant E413DY705hTyr was prepared, but no electrophysiological responses were seen. Studies involving anti-NR2B receptor antibody labeling established that receptors were not trafficked to the surface of the oocytes (Figure 3.20), thwarting efforts to evaluate this double mutant.

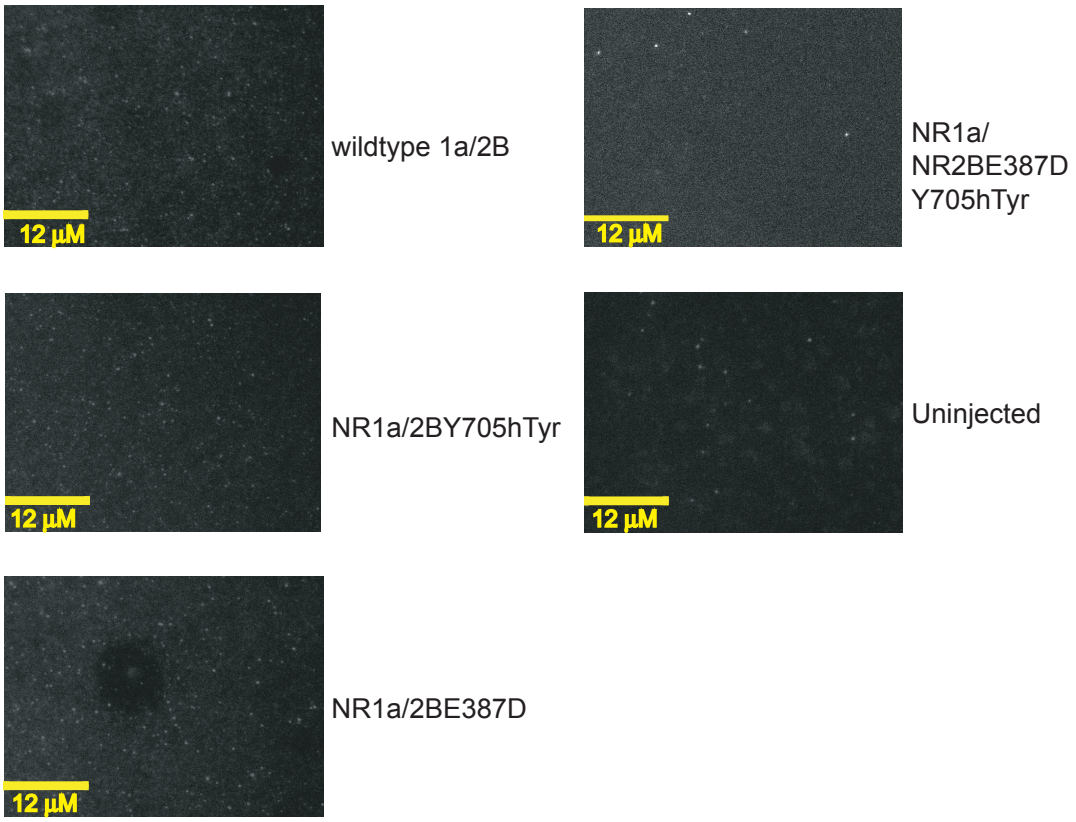

Figure 3.20 TIRF images of *Xenopus laevis* oocytes injected with wild type and mutant NMDA receptors. NR2B antibodies were used to label the NMDA receptors on the oocyte membranes.

3.2.4 Inter-domain Contacts and Mutations in the Glycine-Binding NR1 Subunit

There are many structural differences between the NR2 and NR1 subunits of the NMDA receptor. In fact, there is approximately a 20% sequence identity between the subunits (*46*), and the currently available structural information about NR1 does not correlate as well with the previously mentioned GluR2 structures as the NR2 structures do. Additionally, previous studies of the NR1 ligand binding domain in complex with full and partial agonists suggest that cleft closure around the agonist does not correlate with agonist activity. However, studies with an antagonist, cycloleucine, suggest that an open-cleft conformation contributes to receptor inactivation, similar to studies performed on the AMPA receptor formed from homomeric GluR2 (*39*). Clearly, there is not much consensus on the mechanism relating NR1 partial agonism to channel activation. Previous structural studies of NR1, the glycine binding subunit, suggested that the

clamshell effect was much less pronounced. As noted above, the homology between NR1 and NR2 subunits is not high, and certainly glycine and glutamate are structurally quite different. As such, we felt that applying the unnatural amino acid approach, lengthening amino acid side chains in the NR1 subunit, would provide a good test of the method and an opportunity to confirm previous structural studies.

The NR1 residues that correspond (based on sequence alignments) to the NR2 hydrogen bonding residues discussed above are Q403 and W731. Responses to the full, co-agonist glycine and the partial co-agonists- ACPC (1-aminocyclopropane-1-carboxylic acid), D-CS (D-cycloserine), and ACBC (1-aminocyclobutane-1-carboxylic acid) (Figure 3.13) were measured for functional NR1a/NR2B receptors containing the NR1 mutations Q403N, Q403E, and W731F (numbering for the mature receptors) always in the presence of 100 μM glutamate (Figure 3.21).

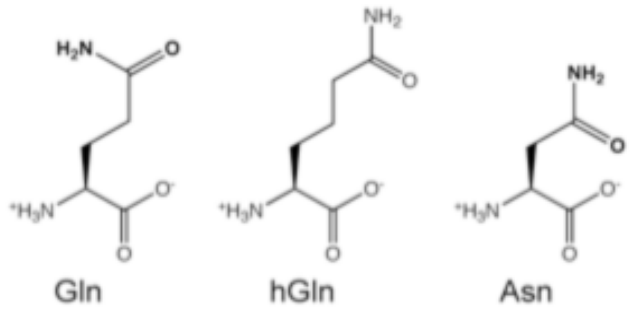

Figure 3.21 Analogs of glutamine (Gln) used in NR1 ligand binding studies, homoglutamate (hGln) and asparagine (Asn).

The ligand-binding domain mutation, Q403N, produced EC_{50} shifts of up to 17-fold (with D-cycloserine and ACPC), suggesting that the length of the side chain in that position of the ligand-binding domain significantly influences receptor activation. The Q403N mutation also influenced the relative efficacies of both D-cycloserine and ACPC, with a slight decrease in relative efficacy being observed for both partial agonists. The mutations introduced at NR1Q403 produced several shifts in relative efficacy for the partial agonist ACBC as well, with a large decrease in overall efficacy observed for the NR1Q403N mutation, without a large shift in EC_{50} (Tables 3.3 and 3.4).

Table 3.3 EC_{50} and relative efficacy for NR1 D1-D2 interface mutations with glycine and (ACPC). Relative efficacy for ACPC is compared to glycine.

Receptor	Glycine EC_{50} ± SEM	Gly Hill	Gly n	ACPC EC_{50} ± SEM	ACPC Hill	ACPC n	ACPC Efficacy
wildtype (1a/2B)	0.98 ± 0.11	1.2 ± 0.13	8	0.28 ± 0.033	1.13± .12	12	0.86±0.011
NR1aQ403N/2B	5.85 ± .13	2.3 ± 0.09	6	4.97 ± .40	1.28 ± 0.081	7	0.27±0.0085
NR1aQ403E/2B	No Current			No Current			
NR1aW731F/2B	4.37 ± .11	2.9 ± 0.19	4	0.43±0.08	1.43 ± .37	5	1.31 ± 0.04
NR1aQ403hGln	5.78±1.058	1.31 ± 0.256	5	1.32 ±0.36	0.74 ± 0.12	6	0.56 ± 0.04

Table 3.4 EC_{50} and relative efficacy for NR1 D1-D2 interface mutations with ACBC and D-cycloserine (D-CS). Relative efficacy for ACBC and D-CS is compared to glycine.

Receptor	ACBC EC_{50} ± SEM	ACBC Hill	ACBC n	ACBC Efficacy
wildtype (1a/2B)	13.9 ± 1.61	1.16 ± 0.12	9	0.43 ± .008
NR1aQ403N	38.3 ±7.1	1.64 ± 0.37	6	0.028 ± 0.0008
NR1aQ403E	25.7±2.4	0.90 ± 0.06	4	0.37 ± 0.011
NR1aW731F	101.59 ± 6.8	1.28 ± 0.09	5	0.87 ± 0.02
NR1aQ403hGln	18.6 ± 7.0	1.13 ± 0.38	6	0.075 ± 0.0033
Receptor	**D-CS EC_{50} ± SEM**	**D-CS Hill**	**D-CS n**	**D-CS Efficacy**
wildtype (1a/2B)	6.02 ± 0.41	1.13 ± 0.08	9	0.66 ± 0.05
NR1aQ403N	99.6 ± 9.19	1.68 ± 0.21	12	0.50 ± 0.018
NR1aQ403E	87.4 ± 4.28	1.89 ± 0.15	5	0.42 ± 0.0197
NR1aW731F	78.8 ± 6.1	1.74 ± 0.18	5	0.57 ± 0.044
NR1aQ403hGln	13.5 ± 2.66	1.06±0.21	5	0.60 ± 0.022

The NR1Q403E mutation produces significant perturbations. The two agonists with the highest efficacy, glycine and ACPC, are no longer agonists for this mutant receptor (Table 3.3). However, the other two partial agonists, D-CS and ACBC, still activate the receptor, with reduced potency. It is possible that the introduction of a negative charge on the side chain and/or the loss of a hydrogen bond donor in the glutamine side chain are important for agonist efficacy (Table 3.4).

Considering the D2 section of the NR1 ligand-binding domain, we evaluated W731F, a relatively severe mutation compared to the others considered here. For this mutant, the functional receptors lost potency with all of the agonists, producing a 5-fold shift for glycine and up to a 14-fold shift with D-CS (Table 3.4). This mutation not only alter the sterics of the side chain, but also removes a hydrogen bond donor. Both of these chemical aspects likely contribute to the decreased potency for all the agonists in the experiment.

3.2.5 Homo-glutamine Incorporation at NR1 Q403

Studies with the conventional mutation Q403N suggested that this site could be a candidate for the "stick in the clam" strategy. In order to probe clamshell closure around different ligands, we incorporated homo-glutamine, hGln, at NR1 Q403. As discussed above, introducing an additional methylene group to the side chain should disrupt clamshell closure. Along with glycine, we considered the three partial agonists, with efficacies at the wild type receptor ranging from 0.43 to 0.86. As shown in Tables 3.3 and 3.4, there is again a correlation between the change in EC_{50} for the hGln mutant and the efficacy of the partial agonist (Figure 3.22, 3.23).

However, it is clear that the NR1 subunit is much less sensitive than the NR2 subunit. The plot in Figure 3.23 reveals that there is indeed a strong correlation between the efficacy of a given agonist on the wild type receptor and the magnitude of the perturbation of EC_{50} induced by the hTyr mutation. As anticipated, the stick in the clam has a larger effect on full agonists, which require full closure, than on partial agonists. In fact, our results demonstrate that it is important to study full-length, functional ion channels especially when trying to determine the molecular-level interactions that govern overall conformational changes in the protein. Additionally, we have demonstrated that our method of studying the functional ion channel is much more sensitive to smaller structural changes that affect the glycine-binding NR1 subunit.

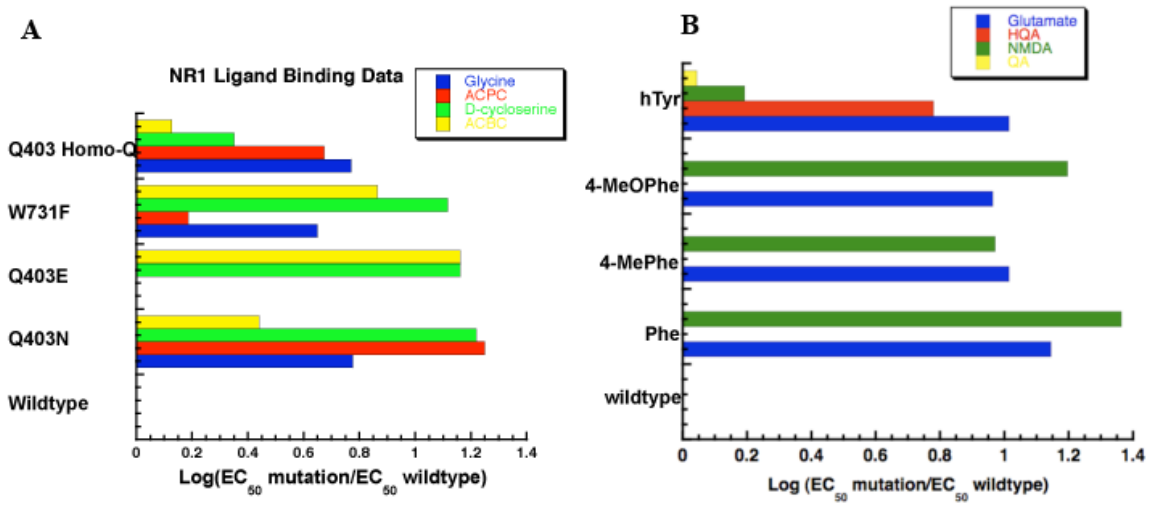

Figure 3.22 Shifts in EC_{50} for each mutant NR1a(A)/NR2B(B) receptor compared to wild type.

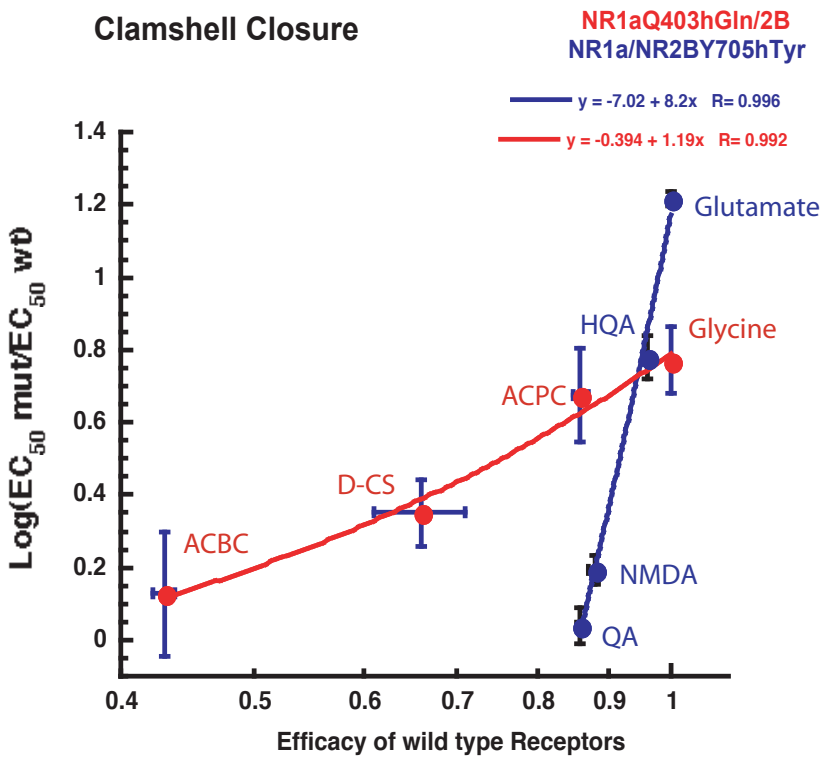

Figure 3.23 The functional probe of clamshell closure: The relationship between partial agonist efficacy for the wild type receptor and Log (EC_{50} responses mut/EC_{50} responses WT) for NR1a/2BY705hTyr and NR1aQ403hGln/NR2B receptors. The relationship between relative efficacy and Log (EC_{50} ratios) demonstrates a measurable energetic relationship between clamshell closure and agonist efficacy. The steepness of the slope is related to the degree of clamshell closure.

3.2.6 GluR2 Structural Study Correlation

The experimental results obtained from the study of the NMDAR binding sites are supported by the available structural data on the homotetrameric GluR2 (AMPA) receptor. The GluR2 residues E402 and L704 are homologous to Q403 and Y705. Distances were measured between the α-carbons of these residues in GluR2 in structures that were 14.7Å unactivated (apo), 13.3Å partially activated (willardiine (HW) and 12.9Å 5-iodowillardiine (IW)), and 12.5Å fully activated (glutamate-bound) (Figure 3.24). From the apo to the glutamate bound structure, as the relative efficacy of the agonist increased, the distance between the α-carbons of E402 and L704 decreased (Figure 3.24). Additionally, the NR2A/glutamate and GluR2/glutamate structures were overlaid, and the

relevant C_α-C_α distances for the two glutamate-bound structures are very similar. Therefore, we feel justified in relating our functional studies on the NMDA receptor to the structural studies of GluR2.

Structure	Cα E402- Cα L704 (GluR2)
GluR2_glutamate	12.53 Å
GluR2_HW	12.86 Å
GluR2_IW	13.31 Å
GluR2_apo	14.73 Å
NR2A_glutamate	12.88 Å

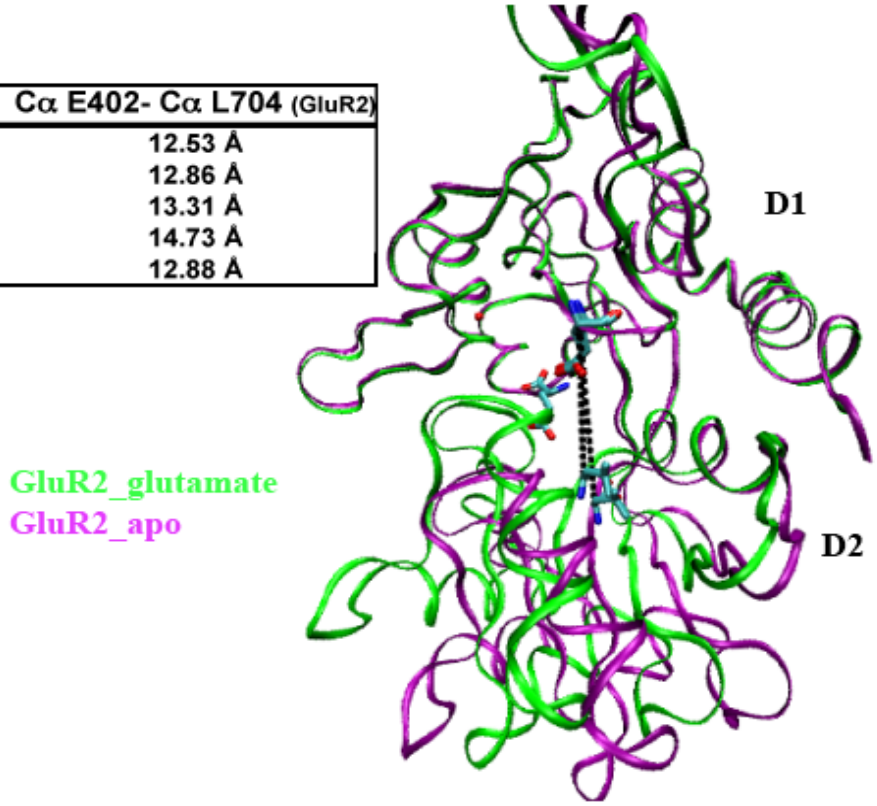

Figure 3.24 Distances between alpha carbons of E402 and L704 in various GluR2 structures (data from PDB files, 1FTJ, IMQJ, 1MQG, 1FTO, and 2A5S). E402 and L704 in GluR2 are homologous to NR2B E387 and Y705. Efficacy values from Jin, *et al.* (*32*).

3.2.7 Implications for the Functional Study of the Clamshell Mechanism of Agonist Action

The most compelling structural studies of clamshell closure have been performed in the homotetrameric AMPA and kainate receptors. It is not clear, however, the extent to which observations for one member of a large class of receptors will apply to all the members of the superfamily. In these studies, we sought an alternative way to evaluate the clamshell mechanism seen in select iGluRs with several specific aims. First, although

there is no denying the compelling images produced by structural biology, there is always value in having complementary functional studies on intact receptors in biologically relevant environments. Secondly, functional measurements allow for the study of a wider range of structures than lower throughput crystallographic approaches. This also allows us to address the third issue related to the risks of extrapolating mechanistic insights from one receptor to all the members of the family.

Conceptually, the approach is straightforward. We engineer into the hinge region of the clamshell a partial occlusion that will prevent full closure. A full agonist, that requires full closure for maximal activation, should be quite sensitive to such an effect. However, such a change should have a lesser impact on a partial agonist, which does not require full clamshell closure to reach its maximum in activation. The approach relies on the power of the nonsense suppression method for site-specifically incorporating unnatural amino acids into receptors and ion channels expressed in vertebrate cells. The subtlety and control that the method enables are essential to producing meaningful results.

The goal of the method was to produce a plot as in Figure 21. We would expect to see a clear correlation between GluR2 function and agonist efficacy, similar to that observed for both NMDA subunits. Here the x-axis is *identical* to that used in the structural studies, the innate efficacy of the agonist on the wild type receptor. But for the y-axis, instead of a structural measure – a distance – we employ a measure of receptor function. If the mechanistic model implied by the GluR2 structural studies is correct, the structural changes must be accompanied by a comparable functional change. The functional measure we use, EC_{50}, is a composite number that reflects both agonist binding and channel gating. The present analysis assumes that, for the sites considered here, mutations affect EC_{50} primarily through changes in gating behavior. Earlier mutagenesis studies (*41*) of these residues and their analogues in other receptors have reached just this conclusion.

Our strategy was to introduce homo-tyrosine, hTyr, at position 705. As illustrated in Figure 3.25, the added CH_2 of hTyr extends the chain and can significantly expand the effective size of the residue depending on the side chain geometry. The addition of a

methylene group may not appear to be that significant at first glance, however, depending on the adopted side chain geometry, a difference in several angstroms exists between the Tyr and hTyr (Figure 3.25). The difference that this methylene unit makes would be the "stick" that would block clamshell closure. It should be noted that all the functionality of the natural residue Tyr is present; it has just been repositioned. The unnatural amino acid hTyr was well-tolerated in the receptor (Figure 3.25), and it produced intriguing results. As shown in Tables 3.1 and 3.2, the effect on EC_{50} ranged from ~17-fold for glutamate to essentially no effect for the partial agonist quinolinic acid (QA). Introduction of a similar residue, homo-glutamine, at NR1Q403, produced a similar result, although the magnitude of the perturbation was attenuated compared to that of hTyr.

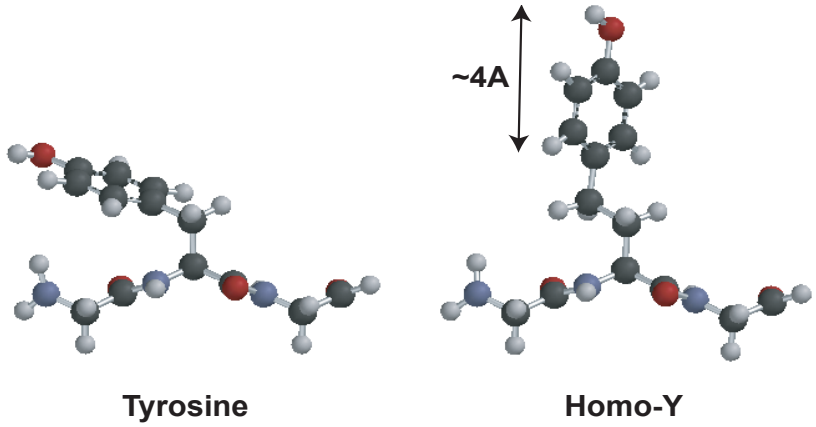

Figure 3.25 Side chain geometries of Tyr and hTyr minimized in GYG/GhTyrG peptides.

Our functional method has resulted in a new probe of the clamshell. By expanding the size of a specific amino acid side chain, while keeping all functionality the same, the importance of a clamshell-like domain closure can be probed. This "stick-in-the-clam" approach using the one-carbon homologue of the natural amino acid should be more consequential for full agonists – which require full clamshell closure – than for partial agonists, which require only partial closure. We find for the glutamate-binding NR2 domain of the NMDA receptor a very strong correlation between agonist efficacy and the impact of the homologation experiment. A similar correlation was observed for

the glycine-binding NR1 domain, however, now the slope is *much* smaller, suggesting that clamshell closure of the NR1 subunit is less critical to receptor function than it is in the NR2 subunit. This, of course, agrees with structural studies, which found no effect in the NR1 subunit. The non-zero slope of Figure 3.23 suggests that perhaps there is a small but significant clamshell effect in NR1, but one that may be too subtle to be revealed in the crystal structures. These results are intriguing, particularly because they suggest that glycine-binding subunits use an attenuated version of the clamshell mechanism to induce structural changes correlating to ion channel activation. More importantly though, along with providing valuable insights into the function of the NMDA receptor, this work introduces a potentially generalizable strategy for probing structural changes associated with receptor activation.

3.3 AMPA Receptor Ligand-Binding Domain Studies

In order to test the generality of our new functional test of the clamshell mechanism in iGluRs, we decided to expand our repertoire of glutamate receptor studies to the homomeric GluR2 receptor. Our goal was to use the nonsense suppression methodology to incorporate the $-CH_2$ elongated amino acid residues that lie at the interdomain hinge region of the ligand binding site. Based on previous GluR2 structural studies, we hypothesized that we would obtain a similar trend as observed above in the NR2BY705 studies. Our studies will parallel those performed by Gouaux and co-workers with the partial agonist series of substituted willardiines.

We acquired the GluR2 construct containing the "flip" sequence. The flip/flop sequence is an alternatively spliced exon consisting of 38 amino acids just prior to the final transmembrane domain and is involved in determining receptor kinetics (*47, 48*). We also use a GluR2 construct containing the unedited glutamine at the Q/R site, which determines the Ca^{2+} permeability of the receptor. The Q-containing receptor is Ca^{2+} permeable. The GluR2 construct also contains the mutation L483Y (504 in the immature protein). This is a non-desensitizing mutation that is thought to stabilize the closed-cleft ligand binding domain (*24, 49*). Our construct is a non-desensitizing, Ca^{2+} permeable GluR2 subunit that forms homotetrameric ion channels.

3.3.1 Mutational Probe of the GluR2 Clamshell

We began our GluR2 investigations by testing the wild type receptor response to glutamate (Figure 3.26). For consistency, we decided to mutate the D1 and D2 amino acids that corresponded to those in our previous NR1 and NR2B studies (Figure 3.15). The corresponding GluR2 D1 amino acid is E402 (mature protein numbering) and the D2 amino acid is not a tyrosine, but L704. These two amino acids cannot interact via a hydrogen bond as in NR2B, but if our hypothesis is based on the size of the amino acid side chain and its ability to "put a stick in the clam," then our method should work for the GluR2 receptor.

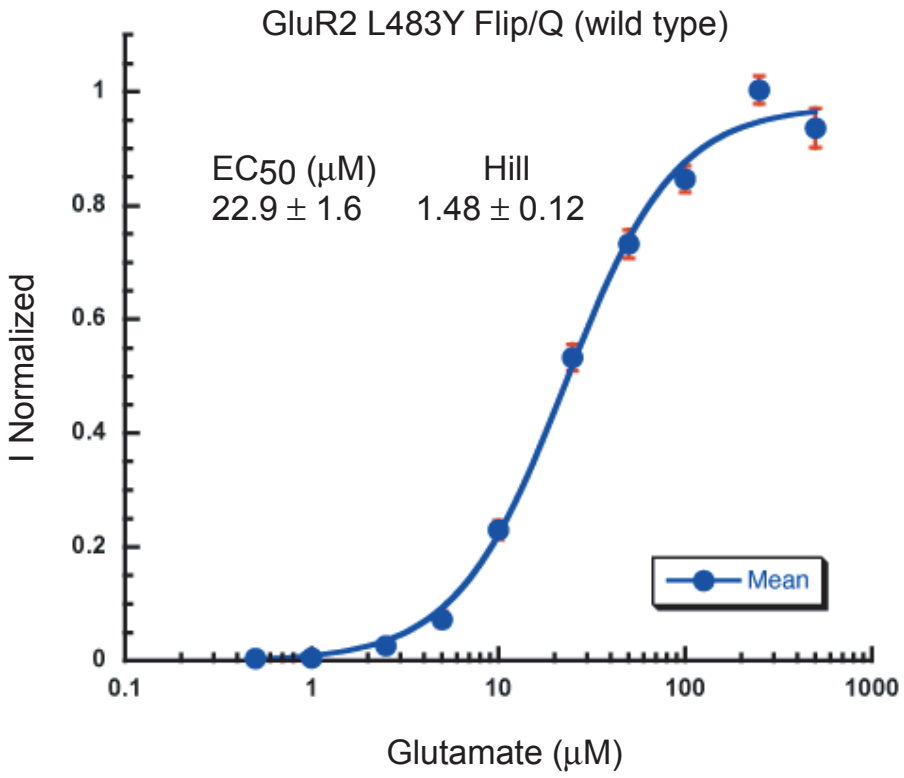

Figure 3.26 Dose-response relationship obtained for wild type GluR2 homomeric channels in response to glutamate.

The first mutations we introduced into GluR2 were at E402- Asp, Asn, homoglutamine (hGln), and nitrohomoalanine (Nha). hGln was incorporated into the

receptor instead of hGlu due to synthetic availability. We also made the L704A mutation, which we felt was appropriately different from Leu in that it is a sterically, much smaller amino acid, but still hydrophobic. One goal of this study was to determine the EC_{50} and efficacy sensitivity of the full and partial agonists at these sites upon mutagenesis. We first recorded responses of all of the homomeric GluR2 receptors to glutamate (Table 3.5).

Table 3.5 EC_{50} values and Hill coefficents for homomeric GluR2 AMPA receptors (n= number of oocytes).

Receptor	Glutamate **EC_{50} ± S.E.M.**	Glutamate **Hill**	Glutamate **n**
wildtype GluR2 (L483Y)	22.3 ± 1.16	1.4 ± .08	11
E402D	20.9 ± 1.81	1.62 ± 0.18	5
E402N	246 ± 21	1.9± 0.21	9
E402TAG hGln	2020 ± 1060	0.90 ± 0.18	20
E402TAG Nha	>3000 ± 1060	0.58 ± 0.16	8
L704A	5.47 ± 0.31	1.91 ± 0.19	13

Not surprisingly, the conservative mutation from Glu to Asp at GluR2402 resulted in no shift in EC_{50} value; however, the mutation to Asn resulted in a ~20-fold shift in EC_{50} (Table 3.5). Clearly, the negatively charged side chain at position 402 is required for proper interaction with the agonist. We also incorporated the unnatural amino acids homoglutamine (hGln) and nitrohomoalanine (Nha), which expanded the Gln side chain by one methylene group (in the case of hGln) and neutralized the charge on the side chain of Glu with an isosteric nitro group (in the case of Nha). Both of these mutations drastically shifted EC_{50} by ~100-fold, indicating glutamate is very sensitive to the charge and the size of the amino acid at this position of the GluR2 binding site. Previous studies have also indicated that mutation of E402 results in shifts in EC_{50} values and glutamate affinity (*26, 50-53*). These studies suggest that E402 is involved in an inter-domain hydrogen bond with Thr686. The stability of clamshell closure around the agonist is directly correlated with the affinity of the agonist. We also made the conventional mutation L402A, which maintains the hydrophobicity of the side chain, but reduces the size. A little surprisingly, this mutation appears to increase agonist affinity and reduces

EC_{50} by ~3.5-fold. It is possible that the smaller side chain, L402A, allows glutamate to fit into the binding site and make more favorable interactions with the receptor.

In order to study the effects of these mutations on partial agonism, we decided to use the willardiine series of partial agonists that were used in the structural studies of GluR2 (Figure 3.9). In addition to the structural work, studies of willardiine action at the GluR2 subunit have been examined using FRET (fluorescence resonance energy transfer) analysis (*54*). The FRET studies determined that the interactions between the LBD and the α-amine group of the agonist contributed to clamshell closure, however this is probably not the only contributing factor. According to the previous GluR2 ligand binding domain studies, the order of partial agonism affinity for the willardiines is: HW~FW>ClW> IW, with HW, FW, ClW, and IW producing 62%, 60%, 53%, and 24% of the currents produced by glutamate, respectively. Overall, this trend follows that as the size of the 5-substituent increases, ion channel activation decreases (*33, 54*).

Table 3.6 EC_{50} values and efficacy measurements for the willardiines in GluR2 receptors. Efficacy measurements are always compared to the full agonist, glutamate. (SEM = standard error measurment)

Receptor	5-FW **EC_{50} ± SEM**	5-FW **Hill**	5-FW **n**	5-FW Efficacy ± SEM
wildtype GluR2 (L483Y)	0.44 ± 0.031	1.79 ± 0.20	14	0.984 ± 0.028
E402D	0.97 ± .112	1.34 ± 0.154	7	0.943 ± 0.047
E402N	1.32 ± 0.024	1.75± 0.04	7	0.998 ± 0.013
E402TAG hGlu	0.15 ± 0.016	1.43 ± 0.17	1	
L704A	0.098 ± 0.005	1.74 ± 0.13	12	0.913 ± 0.0093
Receptor	(S)-HW **EC_{50} ± SEM**	(S)-HW **Hill**	(S)-HW **n**	(S)-HW Efficacy ± SEM
wildtype GluR2 (L483Y)	15.80 ± 0.33	1.94 ± 0.06	13	0.936 ± 0.014
E402D	57.9 ± 10.7	1.25 ± 0.17	11	0.922 ± 0.073
E402N	No Current	No Current	8	0.0 ± 0.016
L704A	8.24 ± 0.355	1.44 ± 0.0753	12	0.936 ± 0.012
Receptor	5-CW **EC_{50} ± SEM**	5-CW **Hill**	5-CW **n**	5-CW Efficacy ± SEM
wildtype GluR2 (L483Y)	1.323 ± 0.053	1.321 ± 0.056	13	0.617 ± 0.010
E402D	5.864 ± 1.171	0.873 ± 0.111	7	0.716 ± 0.020
E402N	76.89 ± 8.60	1.521 ± 0.151	5	0.501 ± 0.016
L704A	1.018 ± 0.13	1.141 ± 0.139	6	1.365 ± 0.126
Receptor	5-IW **EC_{50} ± SEM**	5-IW **Hill**	5-IW **n**	5-IW Efficacy ± SEM
wildtype GluR2 (L483Y)	4.11 ± 0.28	1.63 ± 0.15	16	0.34 ± 0.005
E402D	13.64 ± 1.08	1.55 ± 0.11	11	0.46 ± 0.008
E402N	115.6 ± 80.0	1.30 ± 0.143	8	0.097 ± 0.010
L704A	4.51 ± 0.29	1.37± 0.09	8	0.57 ± 0.012

Our results are summarized in Table 6, and demonstrate a similar trend for the willardiine series, with 5-HW~5-FW > 5-ClW > 5-IW at wild type GluR2 receptors. The mutations at E402 do not drastically shift efficacy for any of the willardiines, however several of the EC_{50} values do shift. The E402N mutation results in ~70-fold shift in EC_{50} for 5-ClW, yet efficacy only decreases slightly (Table 3.6). Our results indicate that these conventional mutations are implicated in the affinity of ligand binding to GluR2 more than they are implicated in ion channel activation. Alternatively, since relative efficacy is measured for each partial agonist against glutamate, and the conformation of

the closed cleft conformation depends on the mutation and not the agonist, the effects on agonist affinity would be evident by EC_{50}, but the relative efficacy would not change because it reflects the effect that the mutation has on both glutamate and the partial agonist.

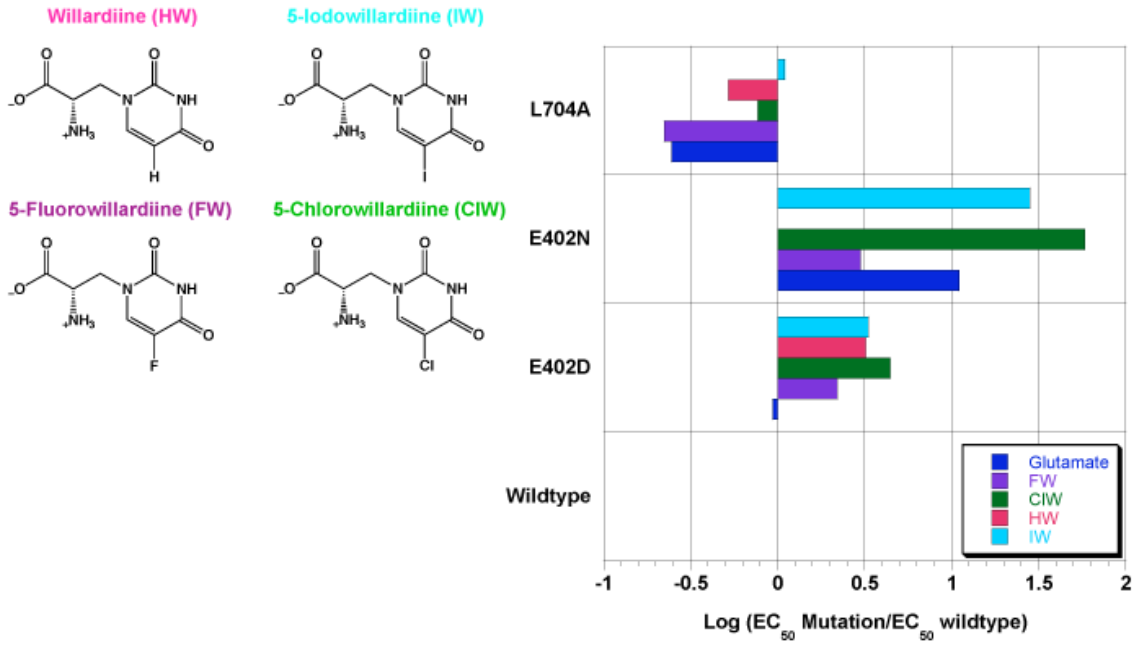

Figure 3.27 Shifts in EC_{50} values for mutations in the GluR2 ligand binding domain with the willardiine partial agonists.

Overall, our first studies of the GluR2 binding site are intriguing in that all of the partial agonists, except for 5-IW, respond more favorably to the L704A mutation (Figure 3.27). This is likely due to the positioning of the 5-substituent on the willardiines, which the alanine mutation can accommodate more easily than the leucine side chain. There is precedent for this type of accommodation where previous structural evidence has demonstrated that a GluR2 methionine side chain, M708, swings out of the binding cleft to prevent a steric clash with 5-IW (*32*). Additionally, our results demonstrate larger EC_{50} increases for the asparagine mutation versus the aspartate mutation; so clearly, maintaining the charge at E402 is necessary for optimal agonist binding.

Our initial studies incorporating the unnatural amino acids, hGln and Nha, at GluR2 E402, resulted in significant EC_{50} shifts for glutamate (Table 3.5) of approximately 100-fold. These measurements become difficult to accurately determine since we have to use very large concentrations of glutamate in order to get full receptor activation. Further studies by a new lab member, Maggie Thompson, using the willardiine partial agonists in combination with hGln and hGlu will determine if our model for the clamshell mechanism of iGluR activation is upheld in the GluR2 receptor.

3.3.2 Studies of Ligand Binding Domain Hinge Residues Involved in Receptor Activation

Studies of the stability of the ligand binding domain dimer, measured by equilibrium centrifugation, correlate with the degree of desensitization of the ion channel (*55*). As the stability of the ligand-binding domain dimer increases, the amount of receptor desensitization decreases. These observations have led to the proposal that a rearrangement of the dimer conformation is required for desensitization to occur (*55*). Further mutational analysis found the non-desensitizing mutation, GluR2L483Y, an interfacial residue thought to stabilize the dimer through a potential cation-π interaction. Corresponding mutations have also been identified in the GluR3 and GluR6 subunits as well (*56, 57*).

In GluR2, the suggested binding partners for the L483Y mutation are L748 and K752. In GluR2, L/Y483 interacts with K752 across the dimer interface. This is the non-desensitizing mutation that we use for our wild type GluR2 receptor. However, we thought that by using the nonsense suppression methodology, we could subtly probe the residues at the dimer-dimer interface to determine the chemical-scale interactions that contribute to dimer stability. We began by studying L/Y483 and incorporating a series of unnatural amino acids that would probe the nature of the proposed electrostatic and or hydrophobic interaction at this site. We incorporated Phe (both with conventional mutagenesis and nonsense suppression), 4-Me-Phe, 4-MeO-Phe, and Cha. We expected that both the kinetics and potency of the agonist could be altered by the mutations.

Table 3.7 EC_{50} values for mutations at GluR2L/Y483 (S.E.M.= standard error measurements).

Receptor	Glutamate **EC_{50} μM ± SEM**	Glutamate **Hill**	Glutamate **N**
wildtype GluR2 (L483Y)	22.3 ± 1.16	1.4 ± .08	11
Y483F	47.6 ± 5.6	1.2 ± .19	14
Y483TAG Phe-THG73	60.4 ± 6.2	1.4 ± 0.19	12
Y483 4-Me-Phe	33.5 ± 5.4	1.8 ± .48	10
Y483 4-MeO-Phe	107 ± 21	1.2 ± .23	10
Y483 Cha	>2500		5

Our initial studies show an ~2-fold shift when Phe is incorporated at this site. Interestingly, eliminating the 4-position hydroxyl group doesn't drastically alter EC_{50}. Additionally, replacing the hydroxyl group with a methyl (4-Me-Phe) produces results similar to the wild type receptor and adding the methoxy group (4-MeO-Phe) increases EC_{50} ~5-fold. The largest shift in EC_{50} value was observed for the Cha mutation, which results in an almost non-functional receptor (Table 3.7).

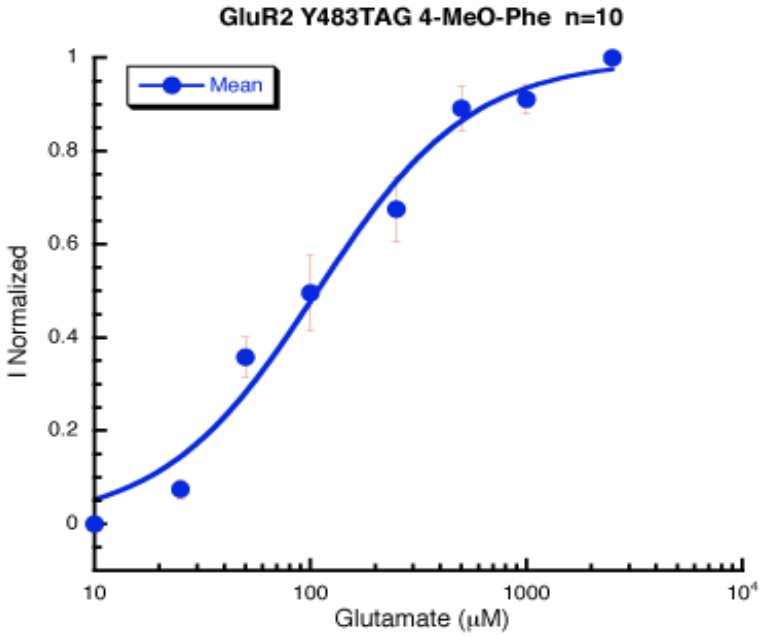

Figure 3.28 Dose-response curve for glutamate at the GluR2 Y483 4-MeO-Phe mutant.

Based on our first observations with unnatural amino acid mutagenesis at the L/Y483 site and using previous knowledge that this site possibly interacts with the hydrophobic L748 and the positively charged K752, we can infer that there are hydrophobic and or electrostatic interactions at the dimer-dimer interface. If a cation-π interaction were involved between Y783 and K752, we would expect to see the largest shift with the Cha mutation. In fact, we see the expected outcome, where mutation to a side chain with similar sterics to Phe but no aromatic component, results in an ~100-fold shift in EC_{50}. In addition, the shift in EC_{50} obtained with the 4-MeO-Phe analog is somewhat expected since the oxygen would draw electron density out of the aromatic ring, reducing its cation-π binding ability with the positively charged lysine (Table 3.7).

Although these results are preliminary, they are suggestive of the power of the unnatural amino acid mutagenesis to determine the chemical-scale interactions involved in regulating the function of iGluRs. We have established a method for unnatural amino acid incorporation into several iGluR receptors and further work in the group by Maggie Thompson will continue to evaluate the ligand-binding domain of GluR2 AMPARs.

3.4 Conclusions and Future Work

We have demonstrated that we are able to incorporate unnatural amino acids into both the NMDA and AMPA families of iGluRs. We have also introduced a new probe of receptor function that utilizes unnatural amino acid mutagenesis. We expanded the side chains of NR2BY705 and NR1aE403 and demonstrated that clamshell-like domain closure around an agonist is more important for full agonists and less so for partial agonists, which required only partial domain closure. We find for the glutamate-binding NR2 domain of the NMDA receptor a very strong correlation between agonist efficacy and the impact of the homologation experiment. This provides a *functional* evaluation of the clamshell mechanism. Interestingly, the analogous experiment performed on the glycine-binding NR1 domain shows a much weaker correlation. These results are consistent with current structural studies and demonstrate a more precise probe of partial agonist action, particularly with the NR1 subunit. Along with providing valuable insights into the

function of the NMDA receptor, this work introduces a potentially generalizable strategy for probing structural changes associated with receptor activation.

In addition, we have begun studies in the AMPA-binding GluR2 receptor. Our initial characterization of interactions in the LBD demonstrates the importance of several residues, i.e., E402 and L704, in determining ligand affinity for the receptor. Additionally, we have evaluated a Tyr mutant (Y483), which lies at the dimer-dimer interface within the ligand binding domain of GluR2 and alters ion channel kinetics resulting in a non-desensitizing receptor. Our initial experiments at this site indicate a potential cation-π interaction with a positively charged arginine in the complementary ligand binding domain, K752. These experiments suggest that a cation-π interaction introduces enough stability at the LBD dimer interface to stabilize the open channel conformational state of the receptor, preventing a shift to a desensitized state. Continued studies by other lab members will confirm the interactions at the dimer interface. In addition, future studies could examine similar interactions in related iGluRs, such as GluR6 that is a KA receptor, which also contains a homologous non-desensitizing Tyr mutation (*56, 57*). Our studies demonstrate the importance of studying these interactions on the chemical-scale with a precise probe, unnatural amino acids, in combination with functional electrophysiology analysis. We are able to expand our repertoire of investigations to a new family of ion channels, with the potential for many further investigations.

3.5 Methods

3.5.1 Electrophysiology

Stage V-VI *Xenopus laevis* oocytes were injected with 50nL/cell of mRNA/tRNA mixtures. NMDAR subunits are cloned into the pAMV vector as described previously, and the GluR2 subunit was obtained from Dr. Yael Stern-Bach in the pGEMHE expression vector. Oocytes with NMDARs injected were evaluated in a Mg^{2+} and Ca^{2+} free saline solution (96 mM NaCl, 5 mM HEPES, 2 mM KCl, and 1 mM $BaCl_2$). The receptors were activated in a Mg^{2+} and Ca^{2+} free solution containing 10 μM glycine (Aldrich) or 100 μM glutamate (Aldrich) and 100 mM niflumic acid (to reduce activity of

Ca^{2+} activated Cl^- channels, Sigma) depending on the mutations being studied. For oocytes containing AMPARs, we utilized a standard Ca^{2+} free saline solution (96 mM NaCl, 5 mM HEPES, 2 mM KCl, and 1 mM $MgCl_2$). All oocyte recordings were made 48 hours after initial injection in two-electrode voltage clamp mode using the OpusXpress 6000A (Molecular Devices). Solutions were perfused at flow rates of 1 and 4 mL/min during agonist application and 3 mL/min during wash. Data were sampled at 125 Hz and filtered at 50 Hz. Eight oocytes were simultaneously voltage clamped at –60 mV, and dose-response relationships were obtained by delivery of increasing concentrations of L-glutamate, NMDA, homoquinolinic acid, or quinolinic acid in 1 mL aliquots for 15s for the NR2B mutations. Increasing concentrations of glycine, ACPC (Sigma), ACBC (Sigma), and D-cycloserine (Sigma) in 1 mL aliquots for 15s were applied to the NR1 mutations. Increasing concentrations of 5-HW, 5-FW, 5-ClW, and 5-IW were applied to the GluR2 mutations. (*S*)-5-Fluorowillardiine (FW), (*S*)-5-Chlorowillardiine (ClW), and (*S)*-Willardiine (HW) were obtained from Ascent Scientific (Somerset, England, United Kingdom), and (*S*)-5-Iodowillardiine (IW) was obtained from Tocris Bioscience (Ellisville, MO). All agonists were prepared in sterile ddi water and diluted in Mg^{2+}, Ca^{2+} free saline solutions (Ca^{2+} free solutions for GluR2). Additionally, all of the drug solutions were maintained at a pH of 7.5. L-glutamate, glycine, NFA, quinolinic acid, and NMDA were all purchased from Sigma Aldrich RBI. Homoquinolinic acid was purchased from Tocris. The data were analyzed using Clampfit 9.0 software (Axon Instruments).

The Hill equation was used to fit data: $I=I_{max}/(1+(EC_{50}/[A]^{nH}))$, where I is peak current at drug concentration (A), EC_{50} is the concentration of drug that evokes 50% of the maximal response, and n_H is the Hill coefficient. Efficacy values were measured for all agonists relative to the maximal glutamate currents evoked on the same cell. Standard error was calculated for both EC_{50} and relative efficacy values.

3.5.2 Mutagenesis and preparation of cRNA and Unnatural Amino Acid Suppression

Mutant NR2B and NR1 constructs were made following the QuickChange mutagenesis protocol (Stratagene). All mutant and wild type cDNAs were linearized with *NotI*, and

mRNA was synthesized by in vitro runoff transcription using the T7 mMESSAGE mMACHINE kit (Ambion). All NR2B mutant mRNA was injected with wild type NR1a mRNA in a NR1a:NR2B (1:5) ratio. All NR1 mutant mRNA was injected with wild type NR2B mRNA in a NR1a:NR2B (5:2) ratio. Wild type receptors were injected in a NR1a:NR2B (1:1) ratio. Synthetic amino acids were ligated to truncated 74 nt tRNA as described previously (*58*). As a negative control for suppression, dCA was ligated to tRNA and co-injected with mRNA. No currents were observed in these experiments. The aminoacyl tRNA was deprotected by photolysis immediately prior to co-injection with mRNA (*58, 59*). Typically, 5 ng mRNA and 25 ng tRNA-aa were injected into oocytes in a total volume of 50 nL.

3.5.3 Immunolocalization of Wild type and Mutant NMDA Receptors

These experiments were performed by adapting previously reported procedures. *Xenopus laevis* oocytes were injected as reported above. Cells were incubated at 16°C for 2 days. The primary antibody, anti-NMDAR2B (Invitrogen; 0.5 mg/mL dilution in phosphate-buffered saline) was used with the Zenon Rabbit IgG Labeling Kit (Molecular Probes) as per labeling instructions. The cells were incubated with primary antibody for 1 h at room temperature. Cells were washed (3x) with phosphate-buffered saline and stored in Mg^{2+}, Ca^{2+} free saline. Oocytes were placed into a hypertonic solution (96 mM NaCl, 5 mM HEPES, 2 mM KCl, 1 mM $MgCl_2$, 1.8 mM $CaCl_2$, and 200 mM Sucrose) for 10 min and the vitelline membrane was removed with fine tweezers. Alexa-Fluor 488 labeled receptors on the oocyte membrane were analyzed using TIRF microscopy.

3.6 Cited References

1. Dingledine, R., Borges, K., Bowie, D., and Traynelis, S. F. (1999) The glutamate receptor ion channels, *Pharmacol Rev 51*, 7-61.
2. Cull-Candy, S., Brickley, S., and Farrant, M. (2001) NMDA receptor subunits: diversity, development and disease, *Curr Opin Neurobiol 11*, 327-335.
3. Coyle, J. T., Tsai, G., and Goff, D. C. (2002) Ionotropic glutamate receptors as therapeutic targets in schizophrenia, *Curr Drug Targets CNS Neurol Disord 1*, 183-189.
4. Nakazawa, K., Quirk, M. C., Chitwood, R. A., Watanabe, M., Yeckel, M. F., Sun, L. D., Kato, A., Carr, C. A., Johnston, D., Wilson, M. A., and Tonegawa, S. (2002) Requirement for hippocampal CA3 NMDA receptors in associative memory recall, *Science 297*, 211-218.
5. Tsai, G., and Coyle, J. T. (2002) Glutamatergic mechanisms in schizophrenia, *Annu Rev Pharmacol Toxicol 42*, 165-179.
6. Armstrong, N., Sun, Y., Chen, G. Q., and Gouaux, E. (1998) Structure of a glutamate-receptor ligand-binding core in complex with kainate, *Nature 395*, 913-917.
7. Bennett, J. A., and Dingledine, R. (1995) Topology profile for a glutamate receptor: three transmembrane domains and a channel-lining reentrant membrane loop, *Neuron 14*, 373-384.
8. Hollmann, M., Maron, C., and Heinemann, S. (1994) N-glycosylation site tagging suggests a three transmembrane domain topology for the glutamate receptor GluR1, *Neuron 13*, 1331-1343.
9. Wo, Z. G., and Oswald, R. E. (1994) Transmembrane topology of two kainate receptor subunits revealed by N-glycosylation, *Proc Natl Acad Sci U S A 91*, 7154-7158.
10. Wo, Z. G., and Oswald, R. E. (1995) A topological analysis of goldfish kainate receptors predicts three transmembrane segments, *J Biol Chem 270*, 2000-2009.
11. O'Hara, P. J., Sheppard, P. O., Thogersen, H., Venezia, D., Haldeman, B. A., McGrane, V., Houamed, K. M., Thomsen, C., Gilbert, T. L., and Mulvihill, E. R. (1993) The ligand-binding domain in metabotropic glutamate receptors is related to bacterial periplasmic binding proteins, *Neuron 11*, 41-52.
12. Quiocho, F. A., and Ledvina, P. S. (1996) Atomic structure and specificity of bacterial periplasmic receptors for active transport and chemotaxis: variation of common themes, *Mol Microbiol 20*, 17-25.
13. Stern-Bach, Y., Bettler, B., Hartley, M., Sheppard, P. O., O'Hara, P. J., and Heinemann, S. F. (1994) Agonist selectivity of glutamate receptors is specified by two domains structurally related to bacterial amino acid-binding proteins, *Neuron 13*, 1345-1357.
14. Mayer, M. L., and Armstrong, N. (2004) Structure and function of glutamate receptor ion channels, *Annu Rev Physiol 66*, 161-181.
15. Kuusinen, A., Arvola, M., and Keinanen, K. (1995) Molecular dissection of the agonist binding site of an AMPA receptor, *Embo J 14*, 6327-6332.
16. Chen, G. Q., and Gouaux, E. (1997) Overexpression of a glutamate receptor (GluR2) ligand binding domain in Escherichia coli: application of a novel protein folding screen, *Proc Natl Acad Sci U S A 94*, 13431-13436.

17. Chen, G. Q., Sun, Y., Jin, R., and Gouaux, E. (1998) Probing the ligand binding domain of the GluR2 receptor by proteolysis and deletion mutagenesis defines domain boundaries and yields a crystallizable construct, *Protein Sci 7*, 2623-2630.
18. Furukawa, H., and Gouaux, E. (2003) Mechanisms of activation, inhibition and specificity: crystal structures of the NMDA receptor NR1 ligand-binding core, *Embo J 22*, 2873-2885.
19. Furukawa, H., Singh, S. K., Mancusso, R., and Gouaux, E. (2005) Subunit arrangement and function in NMDA receptors, *Nature 438*, 185-192.
20. Mayer, M. L. (2005) Crystal structures of the GluR5 and GluR6 ligand binding cores: molecular mechanisms underlying kainate receptor selectivity, *Neuron 45*, 539-552.
21. Mayer, M. L., Olson, R., and Gouaux, E. (2001) Mechanisms for ligand binding to GluR0 ion channels: crystal structures of the glutamate and serine complexes and a closed apo state, *J Mol Biol 311*, 815-836.
22. Armstrong, N., and Gouaux, E. (2000) Mechanisms for activation and antagonism of an AMPA-sensitive glutamate receptor: crystal structures of the GluR2 ligand binding core, *Neuron 28*, 165-181.
23. McFeeters, R. L., and Oswald, R. E. (2002) Structural mobility of the extracellular ligand-binding core of an ionotropic glutamate receptor. Analysis of NMR relaxation dynamics, *Biochemistry 41*, 10472-10481.
24. Sun, Y. J., Rose, J., Wang, B. C., and Hsiao, C. D. (1998) The structure of glutamine-binding protein complexed with glutamine at 1.94 A resolution: comparisons with other amino acid binding proteins, *J Mol Biol 278*, 219-229.
25. Armstrong, N., Mayer, M., and Gouaux, E. (2003) Tuning activation of the AMPA-sensitive GluR2 ion channel by genetic adjustment of agonist-induced conformational changes, *Proc Natl Acad Sci U S A 100*, 5736-5741.
26. Abele, R., Keinanen, K., and Madden, D. R. (2000) Agonist-induced isomerization in a glutamate receptor ligand-binding domain. A kinetic and mutagenetic analysis, *J Biol Chem 275*, 21355-21363.
27. Wyllie, D. J., and Chen, P. E. (2007) Taking the time to study competitive antagonism, *Br J Pharmacol 150*, 541-551.
28. Hogner, A., Kastrup, J. S., Jin, R., Liljefors, T., Mayer, M. L., Egebjerg, J., Larsen, I. K., and Gouaux, E. (2002) Structural basis for AMPA receptor activation and ligand selectivity: crystal structures of five agonist complexes with the GluR2 ligand-binding core, *J Mol Biol 322*, 93-109.
29. Del Castillo, J., and Katz, B. (1957) Interaction at end-plate receptors between different choline derivatives, *Proc R Soc Lond B Biol Sci 146*, 369-381.
30. Monod, J., Wyman, J., and Changeux, J. P. (1965) On The Nature Of Allosteric Transitions: A Plausible Model, *J Mol Biol 12*, 88-118.
31. Li, J., Zagotta, W. N., and Lester, H. A. (1997) Cyclic nucleotide-gated channels: structural basis of ligand efficacy and allosteric modulation, *Q Rev Biophys 30*, 177-193.
32. Jin, R., Banke, T. G., Mayer, M. L., Traynelis, S. F., and Gouaux, E. (2003) Structural basis for partial agonist action at ionotropic glutamate receptors, *Nat Neurosci 6*, 803-810.

33. Jin, R., Horning, M., Mayer, M. L., and Gouaux, E. (2002) Mechanism of activation and selectivity in a ligand-gated ion channel: structural and functional studies of GluR2 and quisqualate, *Biochemistry 41*, 15635-15643.
34. Chen, P. E., and Wyllie, D. J. (2006) Pharmacological insights obtained from structure-function studies of ionotropic glutamate receptors, *Br J Pharmacol 147*, 839-853.
35. Laurie, D. J., and Seeburg, P. H. (1994) Ligand affinities at recombinant N-methyl-D-aspartate receptors depend on subunit composition, *Eur J Pharmacol 268*, 335-345.
36. Monyer, H., Burnashev, N., Laurie, D. J., Sakmann, B., and Seeburg, P. H. (1994) Developmental and regional expression in the rat brain and functional properties of four NMDA receptors, *Neuron 12*, 529-540.
37. Mayer, M. L. (2006) Glutamate receptors at atomic resolution, *Nature 440*, 456-462.
38. Jin, R., and Gouaux, E. (2003) Probing the function, conformational plasticity, and dimer-dimer contacts of the GluR2 ligand-binding core: studies of 5-substituted willardiines and GluR2 S1S2 in the crystal, *Biochemistry 42*, 5201-5213.
39. Inanobe, A., Furukawa, H., and Gouaux, E. (2005) Mechanism of partial agonist action at the NR1 subunit of NMDA receptors, *Neuron 47*, 71-84.
40. Madden, D. R., Cheng, Q., Thiran, S., Rajan, S., Rigo, F., Keinanen, K., Reinelt, S., Zimmermann, H., and Jayaraman, V. (2004) Stereochemistry of glutamate receptor agonist efficacy: engineering a dual-specificity AMPA/kainate receptor, *Biochemistry 43*, 15838-15844.
41. Laube, B., Hirai, H., Sturgess, M., Betz, H., and Kuhse, J. (1997) Molecular determinants of agonist discrimination by NMDA receptor subunits: analysis of the glutamate binding site on the NR2B subunit, *Neuron 18*, 493-503.
42. Laube, B., Schemm, R., and Betz, H. (2004) Molecular determinants of ligand discrimination in the glutamate-binding pocket of the NMDA receptor, *Neuropharmacology 47*, 994-1007.
43. Cashin, A. L., Torrice, M. M., McMenimen, K. A., Lester, H. A., and Dougherty, D. A. (2007) Chemical-scale studies on the role of a conserved aspartate in preorganizing the agonist binding site of the nicotinic acetylcholine receptor, *Biochemistry 46*, 630-639.
44. Chen, P. E., Geballe, M. T., Stansfeld, P. J., Johnston, A. R., Yuan, H., Jacob, A. L., Snyder, J. P., Traynelis, S. F., and Wyllie, D. J. (2005) Structural features of the glutamate binding site in recombinant NR1/NR2A N-methyl-D-aspartate receptors determined by site-directed mutagenesis and molecular modeling, *Mol Pharmacol 67*, 1470-1484.
45. Sun, A., Lankin, D. C., Hardcastle, K., and Snyder, J. P. (2005) 3-Fluoropiperidines and N-methyl-3-fluoropiperidinium salts: the persistence of axial fluorine, *Chemistry 11*, 1579-1591.
46. Monyer, H., Sprengel, R., Schoepfer, R., Herb, A., Higuchi, M., Lomeli, H., Burnashev, N., Sakmann, B., and Seeburg, P. H. (1992) Heteromeric NMDA receptors: molecular and functional distinction of subtypes, *Science 256*, 1217-1221.

47. Lomeli, H., Mosbacher, J., Melcher, T., Hoger, T., Geiger, J. R., Kuner, T., Monyer, H., Higuchi, M., Bach, A., and Seeburg, P. H. (1994) Control of kinetic properties of AMPA receptor channels by nuclear RNA editing, *Science 266*, 1709-1713.
48. Mosbacher, J., Schoepfer, R., Monyer, H., Burnashev, N., Seeburg, P. H., and Ruppersberg, J. P. (1994) A molecular determinant for submillisecond desensitization in glutamate receptors, *Science 266*, 1059-1062.
49. Hansen, K. B., Yuan, H., and Traynelis, S. F. (2007) Structural aspects of AMPA receptor activation, desensitization and deactivation, *Curr Opin Neurobiol 17*, 281-288.
50. Uchino, S., Sakimura, K., Nagahari, K., and Mishina, M. (1992) Mutations in a putative agonist binding region of the AMPA-selective glutamate receptor channel, *FEBS Lett 308*, 253-257.
51. Lampinen, M., Pentikainen, O., Johnson, M. S., and Keinanen, K. (1998) AMPA receptors and bacterial periplasmic amino acid-binding proteins share the ionic mechanism of ligand recognition, *Embo J 17*, 4704-4711.
52. Mano, I., Lamed, Y., and Teichberg, V. I. (1996) A venus flytrap mechanism for activation and desensitization of alpha-amino-3-hydroxy-5-methyl-4-isoxazole propionic acid receptors, *J Biol Chem 271*, 15299-15302.
53. Robert, A., Armstrong, N., Gouaux, J. E., and Howe, J. R. (2005) AMPA receptor binding cleft mutations that alter affinity, efficacy, and recovery from desensitization, *J Neurosci 25*, 3752-3762.
54. Mankiewicz, K. A., Rambhadran, A., Wathen, L., and Jayaraman, V. (2008) Chemical interplay in the mechanism of partial agonist activation in alpha-amino-3-hydroxy-5-methyl-4-isoxazolepropionic acid receptors, *Biochemistry 47*, 398-404.
55. Sun, Y., Olson, R., Horning, M., Armstrong, N., Mayer, M., and Gouaux, E. (2002) Mechanism of glutamate receptor desensitization, *Nature 417*, 245-253.
56. Nanao, M. H., Green, T., Stern-Bach, Y., Heinemann, S. F., and Choe, S. (2005) Structure of the kainate receptor subunit GluR6 agonist-binding domain complexed with domoic acid, *Proc Natl Acad Sci U S A 102*, 1708-1713.
57. Stern-Bach, Y., Russo, S., Neuman, M., and Rosenmund, C. (1998) A point mutation in the glutamate binding site blocks desensitization of AMPA receptors, *Neuron 21*, 907-918.
58. Nowak, M. W., Gallivan, J. P., Silverman, S. K., Labarca, C. G., Dougherty, D. A., and Lester, H. A. (1998) In vivo incorporation of unnatural amino acids into ion channels in Xenopus oocyte expression system, *Methods Enzymol 293*, 504-529.
59. Li, L., Zhong, W., Zacharias, N., Gibbs, C., Lester, H. A., and Dougherty, D. A. (2001) The tethered agonist approach to mapping ion channel proteins--toward a structural model for the agonist binding site of the nicotinic acetylcholine receptor, *Chem Biol 8*, 47-58.